Formation and evolution of a subduction-related mélange: The example of the Rocca Canavese Thrust Sheets (Western Alps)

Manuel Roda[1], Michele Zucali[1], Alessandro Regorda[2] and Maria Iole Spalla[1]

[1]*Università degli Studi di Milano, Dipartimento di Scienze della Terra, Via Mangiagalli 34, 20133 - Milano (Italy)*

[2]*Università degli Studi di Milano, Dipartimento di Scienze della Terra, Via Cicognara 7, 20133 - Milano (Italy)*

ABSTRACT

In the Sesia-Lanzo Zone (SLZ), the Rocca Canavese Thrust Sheets (RCT) subunit is characterized by a mixture of mantle- and crust-derived lithologies, such as metapelites, metagranitoids, metabasics, and serpentinized mantle slices with sizes ranging from meters to hundreds of meters. Structural and metamorphic history suggests that the RCT rocks experienced a complex evolution. In particular, two different peak conditions were obtained for the metabasics, representing different tectono-metamorphic units (TMUs), namely, D1a under eclogite facies conditions and D1b under Lws-blueschist-facies conditions. The two TMUs were coupled during the syn-D2 exhumation stage under Ep-blueschist-facies conditions. The different rocks and metamorphic evolutions and the abundance of serpentinites in the tectonic mixture suggest a possible subduction-related mélange origin for the RCT. To verify whether a subduction-related mélange can record tectono-metamorphic histories similar to that inferred for the RCT, we compare the PT evolutions with the results of a 2D numerical model of ocean-

continent subduction with mantle wedge serpentinization. The predictions of the numerical model fully reproduce the two peak conditions (D1a and D1b) and the successive exhumation history of the two TMUs within the subduction wedge. The degree of mixing estimated from field data is consistent with that predicted by the numerical simulation. Finally, the present-day location of the RCT, which marks the boundary between the orogenic wedge (Penninic and Austroalpine domains) and the southern hinterland (Southalpine domain) of the Alpine chain, is reproduced by the model at the end of the exhumation in the subduction wedge. Therefore, the comparison between natural data and the model results confirms the interpretation of the RCT as a subduction-related mélange occurred during exhumation within a serpentinized mantle wedge.

INTRODUCTION

Mélanges are defined as chaotic bodies of mixed rocks with a block-in-matrix fabric whose internal structure and evolution are intimately linked to the structural, sedimentary, magmatic, and metamorphic processes in the tectonic setting of their formation (Festa et al., 2010, 2012). Subduction-related mélanges form in subduction environments as a result of structural and metamorphic processes; accordingly, they can be described as a tectonic mix of rock units of different sizes (from m- to km-scale), lithologies, origins, ages and metamorphic evolutions enclosed in a highly sheared serpentinite- and/or metasediments-rich matrix (Raymond, 1984; Polino et al., 1990; Federico et al., 2007; Guillot et al., 2009; Cowan, 1985; Malatesta et al., 2012; Roda et al., 2012; Balestro et al., 2015; Wakabayashi, 2015; Ernst, 2016; Roda et al., 2018). Several numerical models highlight the role of the serpentinite-rich matrix in the subduction wedge during the mixing and coupling of blocks of different lithologies and P-T

paths (Gerya et al., 2002; Gerya and Stöckhert, 2005; Guillot et al., 2009; Meda et al., 2010; Malatesta et al., 2012; Roda et al., 2012; Ruh et al., 2015).

Examples of subduction-related mélanges include the Franciscan complex in North America (e.g., Wakabayashi, 2011b, 2011a; Ernst, 2015; Ogawa et al., 2015; Ernst, 2016), the Diahot Unit in New Caledonia (Fitzherbert et al., 2004, 2005), the Rio San Juan Complex in the Dominican Republic (Krebs et al., 2008, 2011), and the Voltri Massif in the Italian Western Alps (Federico et al., 2007; Malatesta et al., 2012; Scarsi et al., 2018). Common features of these mélanges are the occurrence of blocks with different P-T paths recorded within the subduction zone and the serpentinitic nature of the matrix.

As in the previously described complexes, the Rocca Canavese Thrust Sheets (RCT) in the Austroalpine domain of the Western Alps (Fig. 1) consists of a mixture of slices, ranging from meters to hundreds of meters in size, characterized by mantle- and crustal-derived rocks enclosed in a serpentinite-rich matrix (Pognante, 1989a; Spalla and Zulbati, 2003; Barnes et al., 2014; Cantù et al., 2016). The Alps are a double-verging orogen that developed since the Cretaceous as a result of the convergence between Europe and Adria with the subduction of the Alpine Tethys ocean (Ligurian-Piedmont ocean) between the two continental margins (Polino et al., 1990; Spalla et al., 1996; Dal Piaz et al., 2003; Beltrando et al., 2010; Lardeaux, 2014). The Austroalpine domain represents a portion of the Adria plate, buried and exhumed during the oceanic subduction, and now tectonically coupled with the Penninic domain, which represents the oceanic suture zone (e.g., Bousquet et al., 2004; Spalla et al., 2010 and references therein). The Alpine metamorphic history of the RCT accounts for two different peak conditions for the metabasic lenses; one developed under eclogite-facies conditions, and the other developed under Lws-blueschist-facies conditions. Therefore, they are interpreted as two different tectono-

metamorphic units (TMUs; Roda et al., 2018). The serpentinite-rich matrix does not show any of the two peak conditions, but it is characterized by a lower pressure assemblage. The interpretation is that the two TMUs were coupled with the matrix during such lower pressure stage (Roda et al., 2018). The block-in-matrix structural setting, the lithological mixture and the different P-T-d-t paths inferred for the lenses suggest that the RCT rock assemblage is a subduction-related mélange (Roda et al., 2018), analogous to the mélanges described above. However, a comparison between the tectono-metamorphic evolution of the RCT and a numerical model of a subduction system that develops a subduction-related mélange is still lacking.

The aim of this work is to investigate whether the tectono-metamorphic evolution of the RCT can be compared to that of a subduction-related mélange using a 2D numerical model of an ocean-continent subduction zone with serpentinization of the mantle wedge. In particular, we present detailed comparisons between the RCT rock assemblage and the assortment of lithologies represented by numerical markers involved in the subduction wedge and between the metamorphic history inferred for the RCT and that recorded by markers during subduction. We also evaluate the structural setting of the subduction-related mélange at the end of the subduction, and we compare the degree of mixing between the crustal and mantle markers predicted by the model with the actual ratio of crustal and mantle-derived rocks that form the RCT. The mineral abbreviations are after Whitney and Evans (2010).

GEOLOGICAL DATA

Geological setting

The Alps are a subduction-collisional belt that developed since the Cretaceous as a result of the convergence between Europe and Adria. The latter is alternatively considered as a

promontory of Africa or as an independent micro-plate (Dewey et al., 1989; Rosenbaum et al., 2002; Dilek, 2006; Stampfli and Hochard, 2009; Handy et al., 2010). The convergence involved the SSE-dipping subduction of the Alpine Tethys ocean (Ligurian-Piedmont ocean) below Adria plate during the Cretaceous and the subsequent Cenozoic collision of the two continental margins (Polino et al., 1990; Spalla et al., 1996; Dal Piaz et al., 2003; Beltrando et al., 2010; Lardeaux, 2014). The Ligurian-Piedmont ocean originated after the Triassic-Early Jurassic magma-poor rifting between Europa and Adria continents, followed by the Middle to Late Jurassic slow-rate seafloor spreading (Lemoine and Trümpy, 1987; Michard et al., 1996; Manatschal and Müntener, 2009; Saccani et al., 2015; Marotta et al., 2018; Roda et al., 2018; Balestro et al., 2019).

The most external tectonic domain is the European Foreland, which is flexured and underthrust at lithosphere-scale late in the Alpine orogeny, and bounds four main structural domains that are usually distinguished from the external (NW) to the internal (SE) part of the Western Alps (Fig. 1A; e.g., Polino et al., 1990; Dal Piaz et al., 2003; Bousquet et al., 2004; Handy and Oberhänsli, 2004; Schmid et al., 2004). The tectonic setting, lithostratigraphy, pre-Alpine and Alpine evolutions of the domains are described in detail in Table 1. The Helvetic domain, a thick-skinned thrust system of basement rocks and sedimentary cover, results from Cenozoic reactivation, by tectonic inversion of normal faults, which fragmented the European passive margin initially. The Penninic domain is intensely deformed and thermally reactivated since the Cretaceous (early-Alpine) before and during the continental collision and consists of a mixture of thin continental slices and oceanic units (ophiolites from the Ligurian-Piedmont ocean). The ophiolites are characterized by metagabbros, metabasalts and serpentinites, with a geochemical affinity from MORB to subcontinental mantle (Piccardo and Guarnieri, 2010;

Barnes et al., 2014; Rampone et al., 2014; Saccani et al., 2015; Picazo et al., 2016; Zanoni et al., 2016; Luoni et al., 2018; Balestro et al., 2019), and part of them has been interpreted as continental margin ophiolites (Dilek and Furnes, 2011; 2014). The serpentinites represent metasomatized peridotites that were exhumed during continental rifting and subsequent seafloor spreading, although they may locally include intensely hydrated peridotites derived from a mantle wedge (e.g., Federico et al., 2007; Debret et al., 2013). The Austroalpine domain predominantly consists of highly deformed continental rocks derived from the Adria plate, thermally and tectonically reactivated during Alpine subduction-collision-exhumation processes (Gosso, 1977; Lardeaux, 1981; Gosso et al., 1982; Meda et al., 2010; Roda et al., 2012; Lardeaux, 2014). Finally, the Southalpine domain represents the hinterland of the Alpine belt and is a S-verging thick-skinned thrust system involved basement and cover units, only locally imprinted by Alpine metamorphism (Spalla et al., 2014 and references therein).

The RCT is the most internal portion of the Sesia-Lanzo Zone (SLZ; Fig. 1B), which is part of the Austroalpine domain of the Italian Western Alps. The SLZ consists of Paleozoic continental basement rocks (Dal Piaz et al., 1972; Compagnoni et al., 1977) that record pre-Alpine HT metamorphism during the Permian (Lardeaux and Spalla, 1991; Rebay and Spalla, 2001; Schuster and Stüwe, 2008; Spalla et al., 2014). The Alpine evolution was characterized by polyphase deformation under blueschist- to eclogite-facies conditions followed by retrogression under blueschist- to successive greenschist-facies conditions (Compagnoni, 1977; Gosso, 1977; Pognante et al., 1980; Lardeaux et al., 1982; Williams and Compagnoni, 1983; Vuichard, 1987; Lardeaux and Spalla, 1991; Zucali et al., 2002; Gosso et al., 2010; Zucali, 2011; Zucali and Spalla, 2011; Gosso et al., 2015; Corti et al., 2017). The Alpine metamorphic evolution occurred at a low T/depth ratio, which is compatible with oceanic subduction (Cloos, 1993; Handy and

Oberhänsli, 2004; Meda et al., 2010; Roda et al., 2012; Regorda et al., 2017), and these conditions persisted until the exhumation of the SLZ (Spalla et al., 1996; Zucali et al., 2004; Stöckhert and Gerya, 2005; Berger and Bousquet, 2008; Zanoni et al., 2008, 2010; Spalla et al., 2010; Roda et al., 2012).

The SLZ is subdivided into several elements: the Seconda Zona Diorito-Kinzigitica (IIDK), the Gneiss Minuti (GMC) and the Eclogitic Micaschist (EMC) complexes (Dal Piaz et al., 1972; Compagnoni, 1977; Spalla et al., 1983; Pognante, 1989b; Stünitz, 1989; Lardeaux and Spalla, 1991; Wheeler and Butler, 1993; Handy and Oberhänsli, 2004; Babist et al., 2006; Manzotti et al., 2014; Cantù et al., 2016; Corti et al., 2017). The RCT has been recognized as a metamorphic complex that is part of the SLZ (Pognante, 1989a), and it consists of several thrust sheets derived from the pre-Alpine continental crust and upper mantle (Pognante, 1989a, 1989b; Spalla and Zulbati, 2003; Barnes et al., 2014; Roda et al., 2018) that are confined by blueschist-/greenschist-facies mylonitic zones of Alpine age. The RCT is bounded by the EMC to the northwest, the Periadriatic (Canavese) Lineament to the east towards the Southalpine domain, and the Lanzo Massif (LM) to the south (Fig. 1B).

The Southalpine domain is traditionally subdivided into the Ivrea (or Ivrea–Verbano) Zone and the Strona–Ceneri Zone. Alpine deformation was responsible for significant translation and tilting (Brodie et al., 1992; Berger et al., 2012) of the Ivrea Zone, and the metamorphic imprint reached anchizone to low greenschist-facies conditions (Beltrando et al., 2010). Therefore, this portion of the continental margin of the Adria plate was not involved at deep structural levels during Alpine subduction.

Structural and metamorphic evolution of the RCT

The RCT consists of a mixture of mantle- and crust-derived slices composed of metagranitoids and metabasics, with sizes ranging from meters to hundreds of meters, enclosed in a sheared serpentinite- and metapelite-rich matrix (Fig. 1C; Spalla and Zulbati, 2003; Cantù et al., 2016; Roda et al., 2018). Metabasics consist of glaucophanites, metagabbros and minor pyroxenites and omphacitites and may be derived from oceanic or continental protoliths. Metagranitoids and metabasics are characterized by coronitic to mylonitic fabric while serpentinites are generally mylonitic foliated, although some relicts of orthopyroxene, clinopyroxene and spinel can be still detected (Barnes et al., 2014). Four groups of structures and fabric elements have been recognized within the RCT rocks (Pognante, 1989a, 1989b; Spalla and Zulbati, 2003; Cantù et al., 2016; Roda et al., 2018). The first group of structures (D1) consists of a S1 foliation and it is preserved in metapelites and metabasics. In the metagabbros and Jd-bearing glaucophanites, S1 is marked by sodic clinopyroxene, garnet, phengitic mica and epidote. In contrast, in the Lws-bearing glaucophanites, S1 is marked by glaucophane, lawsonite, white mica, garnet and epidote (Roda et al., 2018). Thermobarometric estimates indicate two different peak conditions, for the metabasics (Fig. 2): a) the metagabbros and Jd-bearing glaucophanites experienced a D1a metamorphic stage characterized by pressures of 1.3-1.8 GPa and temperatures of 450-550°C under eclogite-facies conditions; and b) the Lws-bearing glaucophanites experienced a D1b metamorphic stage at temperatures <470°C and pressures of ca. 1.2-1.5 GPa under Lws-blueschist-facies conditions.

The second group of structures (D2) is characterized by a S2 mylonitic foliation, which affects all lithologies and is responsible for the transposition of the original lithostratigraphy, as demonstrated by gabbro boudins within the serpentinites and by glaucophanite lenses within metapelites (Roda et al., 2018). S2 developed under Ep-blueschist-facies conditions (Fig. 2;

P=0.9-1.3 GPa, T=380-500°C), as indicated by the mineral association of glaucophane, garnet, white mica and pumpellyite (Roda et al., 2018). In the serpentinite-rich matrix S2 is marked by Srp and Mag and wraps around clinopyroxene and opaque mineral porphyroclasts, and Chl coronas develop around Mag. Syn-S2 mineral assemblage is compatible with Ep-blueschist-facies conditions (Pognante, 1989a, 1989b; Spalla and Zulbati, 2003; Cantù et al., 2016; Roda et al., 2018). The exhumation from D1a to D2 occurred with decreases in temperature and pressure, whereas the exhumation path from D1b to D2 is characterized by a small increase in temperature (Fig. 2).

The D3 structures are recorded in all lithologies except the metagabbros and consist of centimeter- to meter-scale folding (PA3) of the previous fabric that is associated with an S3 axial plane foliation that developed under greenschist-facies conditions. The D3 imprint coincides with the re-equilibration of previous mineral assemblages in the stability field of chlorite, green amphibole, plagioclase and epidote (Roda et al., 2018). The mineral assemblage is indicative of pressures below 0.9 GPa and temperatures below 380°C (Fig. 2). The D4-related structures are recorded only in the metapelites and consist of a centimeter-spaced crenulation that is locally associated with rough foliation marked by fine-grained chlorite and white mica (Roda et al., 2018).

The tectonic contact between the RCT, the EMC and the LM is characterized by a 100-200-meter-thick mylonitic zone that developed from D2 under blueschist-facies conditions (Spalla and Zulbati, 2003; Cantù et al., 2016; Roda et al., 2018) to D3 under greenschist-facies conditions.

In summary, the RCT is composed of at least two distinct tectono-metamorphic units (TMUs) before D2 (Fig. 2). The first accounts for the exhumation of the metagabbros and Jd-

bearing glaucophanites from eclogite- to Ep-blueschist-facies conditions. The second unit (Lws-bearing glaucophanites), on the other hand, represents the exhumation stage from Lws-blueschist- to Ep-blueschist-facies conditions. The two TMUs were coupled during the exhumation at D2 metamorphic conditions, together with metagranitoids within a serpentinite- and metapelite-rich matrix to form a single TMU, until the final exhumation. The mylonitic zone that marks the tectonic contact between the RCT, the EMC and the LM began forming during D2. The thermal state achieved during the entire metamorphic history is consistent with a P/T ratio for oceanic subduction (Cloos, 1993; Handy and Oberhänsli, 2004; Meda et al., 2010; Roda et al., 2012; Regorda et al., 2017; Roda et al., 2018).

Therefore, the RCT consists of a tectonic mixture of metagabbros, Jd- and Lws-bearing glaucophanites, and metagranitoids different metamorphic histories. They were subsequently incorporated into a serpentinite- and metapelite-rich matrix during D2 deformation phase, reminiscent of other tectonic mélanges described in the literature (e.g., Ernst, 2016; Festa et al., 2019). These features and analogies suggest that the RCT mélange formed within the Alpine subduction wedge (Roda et al., 2018).

NUMERICAL MODELING

Model setup

We used the 2D finite element method to simulate ocean-continent subduction (Regorda et al., 2017) to compare the metamorphic history and lithological heterogeneity of a subduction-related mélange with those that characterize the RCT. The physics of the crust-mantle system during subduction are described by coupled equations for continuity, conservation of momentum and conservation of energy (Marotta et al., 2006). The equations are solved by means of the 2D

finite element code Submar (Marotta et al., 2006), which includes erosion and sedimentation processes (Roda et al., 2012) and oceanic crust dehydration and mantle serpentinization mechanisms (Roda et al., 2010, 2012). According to Regorda et al. (2017), a viscous rheology is assumed for the sublithospheric mantle, and a brittle/plastic rheology is assumed for the lithosphere. The material and rheological parameters used in the simulation are listed in Table 2.

An initial continental lithospheric thickness of 80 km, including 30 km of continental crust, is assumed (Fig. 3) to represent the originally thinned passive margin that characterized the former margin of Adria (Dal Piaz, 2001; Roda et al., 2012; Marotta et al., 2018). An oceanic lithospheric thickness of 80 km is chosen to represent an age of ca. 40 Myr for the Ligure-Piemont Ocean (Handy et al., 2010; Roda et al., 2012) based on the cooling model of a semi-infinite half-space (Turcotte and Schubert, 2002). To simulate plate convergence, a horizontal velocity of 3 cm/yr is imposed along the bottom of the oceanic crust (Roda et al., 2010, 2012). The model runs for 65 Myr of oceanic subduction (from 100 to 35 Ma; Dal Piaz et al., 2003; Handy et al., 2010; Roda et al., 2012). Additional details about the model setup are summarized in the caption of Fig. 3.

Model results

The evolution of the model is similar to other simulations performed with the same code (Roda et al., 2010, 2012; Regorda et al., 2017), and it is consistent with the results obtained with other models of ocean-continent subduction zones (e.g., Gerya and Stöckhert, 2005; Stöckhert and Gerya, 2005; Faccenda et al., 2008; Guillot et al., 2009; Butler et al., 2013) and hydrated subduction wedges (e.g., Billen and Gurnis, 2001; Gerya et al., 2002; Honda and Saito, 2003; Malatesta et al., 2012; Le Voci et al., 2014).

In summary, the subduction of the oceanic lithosphere induces the ablation of the continental crust of the overriding plate because of the strong coupling along the plate boundary. The burial flow involves oceanic and continental crustal material, trench sediments and mantle markers. With the progression of the serpentinization of the mantle wedge (due to the continuous dehydration of the subducting oceanic plate), an intense counterclockwise small-scale convection flow develops in the upper part of the mantle wedge, which causes the exhumation of the subducted material to superficial structural levels, in agreement with the "return flow" model proposed by Cloos (1982, 1986). However, only a small part of the recycled material reaches the surface, and the rest remains in the deeper portion of the mantle wedge or is buried in the sublithospheric mantle. The result is the occurrence of a subduction-related mélange composed of a mixture of exhumed upper and lower oceanic and continental crustal slices, buried and exhumed trench sediments and continental lithospheric mantle enclosed within the serpentinite-rich matrix derived from the hydrated mantle wedge.

The subducted materials record different PT peak conditions, different P-T-t evolutions and different exhumation trajectories, and the size of a single tectono-metamorphic unit ranges from 2-3 km^2 to several tens of km^2, which is consistent with the results discussed by Roda et al. (2012). At the surface, the material involved in the subduction processes (accretion, burial and exhumation) is located in a narrow belt 50-60 km from the trench. The internal part of the upper continental plate (i.e., the hinterland) is not involved in the subduction processes, although it records deformation, resulting in the lateral variation in thickness of the continental crust.

COMPARISON BETWEEN MODEL RESULTS AND GEOLOGICAL DATA

To test whether the reconstructed tectono-metamorphic evolution of the RCT can be reproduced by the numerical model, we extrapolate markers that record PT peak conditions similar to those estimated from the metabasics of the RCT (D1a and D1b, Fig. 2). The origin of these rocks is still under debate and, based on the mineral assemblages, they can be attributed to continental or oceanic crust. Furthermore, the RCT consists of a mixture of metabasics, metapelites and metagranitoids that were coupled during D2 under blueschist-facies conditions (Figs. 1 and 2). For this reason, we extrapolate markers of the continental and oceanic crusts and trench sediments. The discrimination of markers that experienced PT peak conditions comparable to those of D1a and D1b is also based on the peak metamorphic ages. Because no radiometric data are available for this region of the Austroalpine domain, we refer to the interval between 80 and 55 Ma (20-45 Myr of oceanic subduction), such as the time span of the SLZ metamorphic climax (Roda et al., 2012; Regis et al., 2014; Corti et al., 2018; Giuntoli et al., 2018; and references therein). Finally, we compare the evolution of these markers during exhumation within the subduction wedge with the metamorphic history obtained for the RCT rocks (Fig. 2).

The two peak conditions (D1a and D1b) are reproduced well by those of several markers of the oceanic and continental crusts and trench sediments from 20 to 45 Myr of oceanic subduction (Fig. 4). The markers experienced D1a peak conditions and exhume up to D2 conditions (ca. 1.0-1.2 GPa and ca. 400-500°C) isothermally or with a small decrease in temperature (Fig. 4A). In contrast, the exhumation up to D2 conditions of the markers that experienced D1b peak conditions occurs with a gradual small increase in temperature (Fig. 4B). The two groups of markers are coupled at D2 conditions (Fig. 5), and they exhume up to D3 (ca. 0.5-0.8 GPa and ca. 200-300°C) during the successive steps of oceanic subduction (until 65 Myr;

297 i.e., 35 Ma) with gradually decreasing temperature (Fig. 5). Therefore, the entire metamorphic
298 history of the RCT rocks is fully reproduced by the evolution of the markers within the
299 serpentinized subduction wedge.

300 After 65 Myr of subduction (i.e., at 35 Ma), the markers that reproduce the metamorphic
301 history of the RCT form a single tectonic unit composed of slices of continental and oceanic
302 crust and trench sediments (Fig. 6A), which recorded different peak conditions and somewhat
303 different exhumation trajectories (Figs. 4 and 5). The slices are assembled in a narrow strip
304 associated with continental lithospheric mantle and serpentinized mantle that extends from the
305 surface to a depth of ca. 30 km (red area in Fig. 6B). This rock mélange marks the limit between
306 the region that experienced subduction (to the left) and the region that was not involved in the
307 subduction (to the right; Fig. 6B).

308 We also compared the degree of mixing between crustal, sedimentary and mantle
309 materials predicted by the model with the actual ratio of crustal-derived lithotypes and
310 serpentinites that outcrop in the RCT. The amounts of crustal and mantle markers in the tectonic
311 unit (Fig. 6B) at the end of the subduction corresponds to a crust/mantle ratio of 61%. The actual
312 ratio between crustal and mantle-derived materials in the RCT inferred from the geological map
313 (Cantù et al., 2016) is ca. 80%. Thus, the degree of crust-mantle mixing predicted by the model
314 underestimates that obtained from the geological map. However, the estimate derived from the
315 map has a low degree of confidence due to the small percentage of outcrops (less than 10% of
316 the area in the outcrop map of Cantù et al. (2016)). Furthermore, on the geological map, we
317 estimate the degree of mixing in a horizontal direction. In contrast, in the model, we calculate the
318 degree of mixing vertically. Considering these uncertainties, the difference between the two
319 ratios is not significant, and the agreement can be considered acceptable.

DISCUSSION AND CONCLUSIONS

The RCT is characterized by a mixture of mantle- and crust-derived lithologies, such as metagranitoids, metagabbros and glaucophanites blocks, with sizes from meters to hundreds of meters, enclosed in a serpentinite- and metapelite-rich matrix. Geological data suggest a complex metamorphic history for the RCT, which is characterized by two peak conditions for the metabasics, including eclogitic- and Lws-blueschist-facies conditions, both of which indicate thermal states compatible with oceanic subduction. The rocks of the RCT record the first common imprint during D2, which was still under blueschist-facies conditions. Therefore, the coupling between the different blocks and the formation of the tectonic mixture within the serpentinite- and metapelite-rich matrix occurred during the exhumation, under a thermal state compatible with that of a subduction wedge. This suggests that the RCT is a subduction-related mélange, tectonically formed during the exhumation. The two different pre-D2 PT conditions recorded in the metabasics represent the minimum number of contrasting PT evolutions that characterize the RCT mélange. The number of different PT conditions may increase as a result of further detailed petro-structural analyses of the RCT.

Using a numerical model of an ocean-continent subduction zone, we have verified whether a subduction-related mélange can form and evolve within a subduction wedge and whether the metamorphic history of the RCT can be achieved by a subduction-related mélange (Fig. 5). The results of the numerical model indicate that during the subduction of oceanic lithosphere, a mixture of different rocks (oceanic and continental) can coalesce within a serpentinized mantle wedge. The subducted material starts to be exhumed during subduction within the subduction wedge while maintaining a low-temperature state. The materials within the

subduction wedge record different PT peak conditions, different P-T-t evolutions and different exhumation trajectories, and they form a mixture of different tectono-metamorphic units (TMUs) with variable sizes that corresponds to a subduction-related mélange. This scenario is similar to the subduction channel mélange proposed by (Cloos, 1982, 1986) for the Franciscan Complex that accounts for the occurrence of a low viscosity zone of finite width between the lower and upper plate, where a return flow can localize. The low viscosity zone is the result of dehydration of the oceanic crust and consequent hydration and serpentinization of the upper plate mantle (Billen and Gurnis, 2001; Gerya et al., 2002; Hirth and Kohlstedt, 2003; Honda and Saito, 2003). Numerical models, as well seismic and tomographic studies agree with a wedge-shape of the low viscosity zone in the upper plate mantle during the subduction (Billen and Gurnis, 2001; Gerya and Stockhert, 2002; Honda and Saito, 2003; Arcay et al., 2005; Gerya and Stöckhert, 2005; Abers et al., 2006; Rondenay et al., 2008; Roda et al., 2010, 2012; Quinquis and Buiter, 2014; Regorda et al., 2017). Furthermore, the very different P/T ratios and exhumation paths recorded by some rocks during the subduction suggest a larger low viscosity zone than a thin channel (e.g., Roda et al., 2012; Penniston-Dorland et al., 2018). The shape and width of the hydrated mantle wedge (low viscosity zone) can vary with subduction rate, duration of the subduction, thickness of the oceanic plate, thickness of the overriding plate and subduction dip (e.g., Meda et al., 2010; Roda et al., 2010, 2011a, 2012; Regorda et al., 2017). In this scenario, the serpentinite-rich matrix of RCT mélange would derive from the hydrated mantle wedge as proposed for the Voltri Massif (Federico et al., 2007; Malatesta et al., 2012).

The entire tectono-metamorphic history of the RCT is fully reproduced by the evolution of numerical markers within the serpentinized subduction wedge in terms of the lithological mixing, quantitative P-T estimates and exhumation trajectories. Based on the final spatial

366 distribution of markers, the subduction-related mélange was exhumed at the boundary between
367 the zone of mixing of recycled crustal material and variably serpentinized mantle, and the zone
368 with the lithospheric material was never involved in the subduction (Fig. 6). This agrees with the
369 geological setting of the RCT that marks the boundary between the inner, subduction-related,
370 units of the Alpine chain (Penninic and Austroalpine domains) and the outer units, such as the
371 Southalpine domain, which likely acted as the buttress of the subduction system.

372 Based on our comparison of the tectono-metamorphic history of the RCT lithologies with
373 the evolution of crust- and mantle-derived markers within a modeled subduction wedge, we infer
374 that the RCT represents a subduction-related mélange in the Austroalpine domain of the Alps.
375 We depict the time-progressive development of this mélange in a tectonic model diagram in
376 Figure 7. During the subduction of the Ligurian-Piedmont ocean the burial of oceanic,
377 continental and sedimentary rocks occurred (Fig. 7A), subsequently recycled within the hydrated
378 mantle wedge (Fig. 7B). Accordingly, the metabasics blocks of RCT recorded different PT
379 conditions within the mantle wedge (D1a and D1b, Fig. 7B). Subsequently, during the
380 exhumation, they are coupled with other lithologies within a serpentinite-rich matrix (D2
381 metamorphic conditions, Fig. 7C), forming the RTC tectonic mélange. The RTC tectonic
382 mélange exhumed as a single tectono-metamorphic unit (Fig. 7D) until the continental collision
383 of the European plate (Fig. 7E), and now marking the boundary between the orogenic wedge
384 (Austroalpine and Penninic domains), and the southern hinterland of the Alpine belt (Southalpine
385 domain), not involved in the subduction process (Fig. 7F). The orogenic wedge is a tectonic
386 mixture of oceanic and continental rocks buried at different depths and exhumed to crustal
387 levels, with part of the hydrated mantle wedge.
388

ACKNOWLEDGMENTS

The authors acknowledge Linea 2, Azione A - fondi giovani ricercatori “Analisi strutturale delle catene collisionali” (PSR2018_DZANON). We thank Anna Maria Marotta and Francesca de Salvo for helping with the comparison between model predictions and natural data and Guido Gosso for discussion and critical reading of the text. American Journal Expert is thanked for the final English editing. The Associate Editor, an anonymous reviewer and Yildirim Dilek are gratefully acknowledged for their highly constructive criticism of the text.

REFERENCES CITED

Abers, G.A., van Keken, P.E., Kneller, E.A., Ferris, A., and Stachnik, J.C., 2006, The thermal structure of subduction zones constrained by seismic imaging: Implications for slab dehydration and wedge flow: Earth and Planetary Science Letters, v. 241, p. 387–397.

Afonso, J.C., and Ranalli, G., 2004, Crustal and mantle strengths in continental lithosphere: is the jelly sandwich model obsolete? Tectonophysics, v. 394, p. 221–232, doi: 10.1016/j.tecto.2004.08.006.

Arcay, D., Tric, E., and Doin, M.-P., 2005, Numerical simulations of subduction zones: Physics of the Earth and Planetary Interiors, v. 149, p. 133–153, doi: 10.1016/j.pepi.2004.08.020.

Babist, J., Handy, M.R., Konrad-Schmolke, M., and Hammerschmidt, K., 2006, Precollisional, multistage exhumation of subducted continental crust: The Sesia Zone, western Alps: Tectonics, v. 25, doi: 10.1029/2005TC001927.

Balestro, G., Festa, A., and Dilek, Y., 2019, Structural Architecture of the Western Alpine Ophiolites, and the Jurassic Seafloor Spreading Tectonics of the Alpine Tethys: Journal of the Geological Society, p. jgs2018-099, doi: 10.1144/jgs2018-099.

Balestro, G., Festa, A., and Tartarotti, P., 2015, Tectonic significance of different block-in-matrix structures in exhumed convergent plate margins: examples from oceanic and continental HP rocks in Inner Western Alps (northwest Italy): International Geology Review, v. 57, p. 581–605, doi: 10.1080/00206814.2014.943307.

Barnes, J.D., Beltrando, M., Lee, C.-T.A., Cisneros, M., Loewy, S., and Chin, E., 2014, Geochemistry of Alpine serpentinites from rifting to subduction: A view across paleogeographic domains and metamorphic grade: Chemical Geology, v. 389, p. 29–47, doi: 10.1016/j.chemgeo.2014.09.012.

Beltrando, M., Compagnoni, R., and Lombardo, B., 2010, (Ultra-) High-pressure metamorphism and orogenesis: An Alpine perspective: Gondwana Research, v. 18, p. 147–166, doi: 10.1016/j.gr.2010.01.009.

Berger, A., and Bousquet, R., 2008, Subduction-related metamorphism in the Alps: review of isotopic ages based on petrology and their geodynamic consequences: Geological Society, London, Special Publications, v. 298, p. 117–144, doi: 10.1144/SP298.7.

Berger, A., Mercolli, I., Kapferer, N., and Fügenschuh, B., 2012, Single and double exhumation of fault blocks in the internal Sesia-Lanzo Zone and the Ivrea-Verbano Zone (Biella, Italy): International Journal of Earth Sciences, v. 101, p. 1877–1894, doi: 10.1007/s00531-012-0755-6.

Best, M.G., and Christiansen, E.H., 2001, Igneous Petrology: Blackwell Sci., London.

Billen, M.I., and Gurnis, M., 2001, A low viscosity wedge in subduction zones: Earth and Planetary Science Letters, v. 193, p. 227–236.

Bousquet, R., Engi, M., Gosso, G., Oberhänsli, R., Berger, A., Spalla, M.I., Zucali, M., and Goffè, B., 2004, Explanatory notes to the map: metamorphic structure of the Alps transition from the Western to the Central Alps: Mitteilungen der Gesellschaft der Geologie- und Bergbaustudenten in Österreich, v. 149, p. 145–156.

Brack, P., 1981, Structures in the southwestern border of the Adamello intrusion (Alpi Bresciane, Italy): Schweizerische Mineralogische und Petrographische Mitteilungen, v. 61, p. 37–50, doi: 10.5169/seals-47129.

Brodie, K.H., Rutter, E.H., and Evans, P., 1992, On the structure of the Ivrea-Verbano Zone (northern Italy) and its implications for present-day lower continental crust geometry: Terra Nova, v. 4, p. 34–40, doi: 10.1111/j.1365-3121.1992.tb00448.x.

443 Butler, J.P., Beaumont, C., and Jamieson, R.A., 2013, The Alps 1: A working geodynamic model
444 for burial and exhumation of (ultra)high-pressure rocks in Alpine-type orogens: Earth and
445 Planetary Science Letters, v. 377–378, doi: 10.1016/j.epsl.2013.06.039.
446 Cantù, M., Spaggiari, L., Zucali, M., Zanoni, D., and Spalla, M.I., 2016, Structural analysis of a
447 subduction-related contact in southern Sesia-Lanzo Zone (Austroalpine Domain, Italian
448 Western Alps): Journal of Maps, v. 12, p. 22–35, doi: 10.1080/17445647.2016.1155925.
449 Chopra, P.N., and Paterson, M.S., 1981, The experimental deformation of dunite:
450 Tectonophysics, v. 78, p. 453–473, doi: 10.1016/0040-1951(81)90024-X.
451 Cloos, M., 1982, Flow melanges: Numerical modeling and geologic constraints on their origin in
452 the Franciscan subduction complex, California: Geological Society of America Bulletin, v.
453 93, p. 330, doi: 10.1130/0016-7606(1982)93<330:FMNMAG>2.0.CO;2.
454 Cloos, M., 1986, Blueschists in the Franciscan Complex of California: Petrotectonic constraints
455 on uplift mechanisms, *in* Evans, B.W. and Brown, E.H. eds., Blueschists and Eclogites,
456 Geological Society of America, v. 164, p. 77–94, doi: 10.1130/MEM164-p77.
457 Cloos, M., 1993, Lithospheric buoyancy and collisional orogenesis: Subduction of oceanic
458 plateaus, continental margins, island arcs, spreading ridges, and seamounts: Geological
459 Society of America Bulletin, v. 105, p. 715, doi: 10.1130/0016-
460 7606(1993)105<0715:LBACOS>2.3.CO;2.
461 Compagnoni, R., 1977, The Sesia-Lanzo zone: high-pressure low-temperature metamorphism in
462 the Austroalpine continental margin: Rendiconti della Società Italiana di Mineralogia e
463 Petrologia, v. 33, p. 335–374.
464 Compagnoni, R., Dal Piaz, G.V., Hunziker, J.C., Gosso, G., Lombardo, B., and Williams, P.F.,
465 1977, The Sesia-Lanzo Zone, a slice of continental crust with alpine high pressure-low

temperature assemblages in the western Italian Alps: Rendiconti della Società Italiana di Mineralogia e Petrologia, v. 33, p. 281–334.

Corti, L., Alberelli, G., Zanoni, D., and Zucali, M., 2017, Analysis of fabric evolution and metamorphic reaction progress at Lago della Vecchia-Valle d'Irogna, Sesia-Lanzo Zone, Western Alps: Journal of Maps, v. 13, p. 521–533, doi: 10.1080/17445647.2017.1331177.

Corti, L., Alberelli, G., Zanoni, D., and Zucali, M., 2018, Tectonometamorphic evolution of the Lago della Vecchia metaintrusive and its country rocks, Sesia-Lanzo Zone, Western Alps: Italian Journal of Geosciences, v. 137, p. 188–207, doi: 10.3301/IJG.2018.08.

Cowan, D.S., 1985, Structural styles in Mesozoic and Cenozoic mélanges in the western Cordillera of North America: Geological Society of America Bulletin, v. 96, p. 451, doi: 10.1130/0016-7606(1985)96<451:SSIMAC>2.0.CO;2.

Dal Piaz, G.V., 2001, History of tectonic interpretations of the Alps: Journal of Geodynamics, v. 32, p. 99–114, doi: 10.1016/S0264-3707(01)00019-9.

Dal Piaz, G.V., 2010, The Italian Alps: a journey across two centuries of Alpine geology (M. Beltrando, A. Peccerillo, M. Mattei, S. Conticelli, & C. Doglioni, Eds.): Journal of the Virtual Explorer, v. 36, doi: 10.3809/jvirtex.2010.00234.

Dal Piaz, G.V., Bistacchi, A., and Massironi, M., 2003, Geological outline of the Alps: Episodes, v. 26, p. 175–180.

Dal Piaz, G.V., Hunziker, J.C., and Martinotti, G., 1972, La Zona Sesia -- Lanzo e l'evoluzione tettonico-metamorfica delle Alpi Nordoccidentali interne: Memorie della Società Geologica Italiana, v. 11, p. 433–460.

Debret, B., Nicolet, C., Andreani, M., Schwartz, S., and Godard, M., 2013, Three steps of serpentinization in an eclogitized oceanic serpentinization front (Lanzo Massif - Western

489 Alps): Journal of Metamorphic Geology, v. 31, p. 165–186, doi: 10.1111/jmg.12008.
490 Dewey, J.F., Helman, M.L., Turco, E., Hutton, D.H.W., and Knott, S.D., 1989, Kinematics of the
491 western Mediterranean, *in* Coward, M.P., Dietrich, D., and Park, R.G. eds., Alpine
492 tectonics, Geol. Soc. Spe. Pub., London, v. 45, p. 265–283.
493 Dilek, Y., 2006, Collision tectonics of the Mediterranean region: Causes and consequences, *in*
494 Dilek, Y. and Pavlides, S. eds., Postcollisional Tectonics and Magmatism in the
495 Mediterranean Region and Asia, Geological Society of America, v. 409, p. 0, doi:
496 10.1130/2006.2409(01).
497 Dilek, Y and Furnes, H., (2011) Ophiolite genesis and global tectonics: geochemical and tectonic
498 fingerprinting of ancient oceanic lithosphere: The Geological Society of America Bulletin, vol.
499 123, p. 387-411, doi: 10.1130/B30446.1.
500 Dilek, Y., and Furnes, Y., (2014) Origins of ophiolites: Elements, vol. 10, p. 93-100. doi:
501 10.2013/gselements.10.2.93
502 Dubois, J., and Diament, M., 1997, Géophysique: Masson, Paris.
503 England, P.C., and Thompson, A.B., 1984, Pressure--Temperature--Time Paths of Regional
504 Metamorphism I. Heat Transfer during the Evolution of Regions of Thickened Continental
505 Crust: Journal of Petrology, v. 25, p. 894–928, doi: 10.1093/petrology/25.4.894.
506 Ernst, W.G., 1973, Interpretative Synthesis of Metamorphism in the Alps: Geological Society of
507 America Bulletin, v. 84, p. 2053, doi: 10.1130/0016-
508 7606(1973)84<2053:ISOMIT>2.0.CO;2.
509 Ernst, W.G., 2015, Franciscan geologic history constrained by tectonic/olistostromal high-grade
510 metamafic blocks in the iconic California Mesozoic-Cenozoic accretionary complex:
511 American Mineralogist, v. 100, p. 6–13, doi: 10.2138/am-2015-4850.

512 Ernst, W.G., 2016, Franciscan mélanges: coherent blocks in a low-density, ductile matrix:
513 International Geology Review, v. 58, p. 626–642, doi: 10.1080/00206814.2015.1108879.
514 Ernst, W.G., and Liou, J.G., 2008, High- and ultrahigh-pressure metamorphism: Past results and
515 future prospects: American Mineralogist, v. 93, p. 1771–1786, doi: 10.2138/am.2008.2940.
516 Faccenda, M., Gerya, T.V., and Chakraborty, S., 2008, Styles of post-subduction collisional
517 orogeny: Influence of convergence velocity, crustal rheology and radiogenic heat
518 production: Lithos, v. 103, p. 257–287, doi: 10.1016/j.lithos.2007.09.009.
519 Federico, L., Crispini, L., Scambelluri, M., and Capponi, G., 2007, Ophiolite mélange zone
520 records exhumation in a fossil subduction channel: Geology, v. 35, p. 499–502, doi:
521 10.1130/G23190A.1.
522 Festa, A., Dilek, Y., Pini, G.A., Codegone, G., and Ogata, K., 2012, Mechanisms and processes
523 of stratal disruption and mixing in the development of mélanges and broken formations:
524 Redefining and classifying mélanges: Tectonophysics, v. 568–569, p. 7–24, doi:
525 10.1016/j.tecto.2012.05.021.
526 Festa, A., Pini, G.A., Dilek, Y., and Codegone, G., 2010, Mélanges and mélange-forming
527 processes: a historical overview and new concepts: International Geology Review, v. 52, p.
528 1040–1105, doi: 10.1080/00206810903557704.
529 Festa, A., Pini, G.A., Ogata, K., and Dilek, Y., 2019, Diagnostic features and field-criteria in
530 recognition of tectonic, sedimentary and diapiric mélanges in orogenic belts and exhumed
531 subduction-accretion complexes: Gondwana Research, doi: 10.1016/J.GR.2019.01.003.
532 Filippi, M., Gosso, G., Lardeaux, J.-M., Spalla, M.I., Verati, C., and Zanoni, D., 2018, The late-
533 to post-Variscan dioritic dykeswarm of the Argentera- Mercantour massif and its tectono-
534 metamorphic record, *in* Proceedings of the 26th Earth Sciences Meeting of the Société

Géologique de France, p. 167.

Fitzherbert, J.A., Clarke, G.L., Marmo, B., and Powell, R., 2004, The origin and P-T evolution of peridotites and serpentinites of NE New Caledonia: prograde interaction between continental margin and the mantle wedge: J. metamorphic Geol., v. 22, p. 327–344.

Fitzherbert, J.A., Clarke, G.L., and Powell, R., 2005, Preferential retrogression of high-P metasediments and the preservation of blueschist to eclogite facies metabasite during exhumation, Diahot terrane, NE New Caledonia: Lithos, v. 83, p. 67–96, doi: 10.1016/j.lithos.2005.01.005.

Gerya, T.V., and Stockhert, B., 2002, Exhumation rates of high pressure metamorphic rocks in subduction channels: The effect of Rheology.: Geophysical Research Letters, v. 29, p. 1–19, doi: 10.1029/2002TC001406.

Gerya, T.V., and Stöckhert, B., 2005, Two-dimensional numerical modeling of tectonic and metamorphic histories at active continental margins: Int J Earth Sci (Geol Rundsch), v. 95, p. 250–274, doi: 10.1007/s00531-005-0035-9.

Gerya, T.V., Stöckhert, B., and Perchuk, A.L., 2002, Exhumation of high-pressure metamorphic rocks in a subduction channel: A numerical simulation: Tectonics, v. 21, p. 1–15, doi: 10.1029/2002TC001406.

Gerya, T.V., and Yuen, D.A., 2003, Characteristics-based marker-in-cell method with conservative finite-differences schemes for modeling geological flows with strongly variable transport properties: Physics of the Earth and Planetary Interiors, v. 140, p. 293–318, doi: 10.1016/j.pepi.2003.09.006.

Giuntoli, F., Lanari, P., Burn, M., Kunz, B.E., and Engi, M., 2018, Deeply subducted continental fragments – Part 2: Insight from petrochronology in the central Sesia Zone (western Italian

Alps): Solid Earth, v. 9, p. 191–222, doi: 10.5194/se-9-191-2018.

Gosso, G., 1977, Metamorphic evolution and fold history in the eclogite micaschists of the upper Gressoney valley (Sesia-Lanzo zone, Western Alps): Rendiconti della Società Italiana di Mineralogia e Petrologia, v. 33, p. 389–407.

Gosso, G., Kienast, J.R., Lardeaux, J.-M., and Lombardo, B., 1982, Replissement intense et transposition (en climat métamorphique de haute pression) fes contacts tectoniques majeurs dans l'edifice supérieur des nappes alpines (zone Sesia-Lanzo): Compte Rendu Academie des Sciences Paris, v. 294, p. 343–348.

Gosso, G., Messiga, B., Rebay, G., and Spalla, M.I., 2010, The interplay between deformation and metamorphism during eclogitization of amphibolites in the Sesia-Lanzo zone of the Western Alps: International Geology Review, v. 51, p. 1193–1219, doi: 10.1080/00206810903529646.

Gosso, G., Rebay, G., Roda, M., Spalla, M.I., Tarallo, M., Zanoni, D., and Zucali, M., 2015, Taking advantage of petrostructural heterogeneities in subduction- collisional orogens, and effect on the scale of analysis: Periodico di Mineralogia, v. 84, p. 779–825, doi: 10.2451/2015PM0452.

Guillot, S., Hattori, K., Agard, P., Schwartz, S., and Vidal, O., 2009, Exhumation Processes in Oceanic and Continental Subduction Contexts: A Review, *in* Lallemand, S. and Funiciello, F. eds., Subduction Zone Dynamics, Springer-Verlag Berlin Heidelberg, p. 175–204, doi: 10.1007/978-3-540-87974-9.

Haenel, R., Rybach, L., and Stegena, L., 1988, Handbook of Terrestrial Heat-Flow Density Determination: Kluwer Academic Publishers.

Handy, M.R., and Oberhänsli, R., 2004, Explanatory notes to the map: metamorphic structure of

581 the Alps age map of the metamorphic structure of the Alps - tectonic interpretation and
582 outstanding problem: Mitt. Österr. Miner. Ges., v. 149, p. 201–225.
583 Handy, M.R., Schmid, S.M., Bousquet, R., Kissling, E., and Bernoulli, D., 2010, Reconciling
584 plate-tectonic reconstructions of Alpine Tethys with the geological--geophysical record of
585 spreading and subduction in the Alps: Earth-Science Reviews, v. 102, p. 121–158, doi:
586 10.1016/j.earscirev.2010.06.002.
587 Hirth, G., and Kohlstedt, D., 2003, Rheology of the upper mantle and the mantle wedge: A view
588 from the experimentalists, *in* Inside the Subduction Factory, American Geophysical Union
589 (AGU), p. 83–105, doi: 10.1029/138GM06.
590 Honda, S., and Saito, M., 2003, Small-scale convection under the back-arc occurring in the low
591 viscosity wedge: Earth and Planetary Science Letters, v. 216, p. 703–715, doi:
592 10.1016/S0012-821X(03)00537-5.
593 Hunziker, J.C., 1992, Thirty-two years of geochronological work in the Central and Western
594 Alps: a review of seven maps: Memoires de Geologie (Lausanne, Switzerland) Edited by:
595 InterRad Jurassic-Cretaceous Working Group,23ologie. Lau- sanne, v. 13, p. 1–59.
596 Kirby, S.H., 1983, Rheology of the Lithosphere: Review of Geophysics, v. 21, p. 1459–1487,
597 doi: 10.1029/RG021i006p01458.
598 Krebs, M., Maresch, W.V., Schertl, H.-P., Münker, C., Baumann, A., Draper, G., Idleman, B.,
599 and Trapp, E., 2008, The dynamics of intra-oceanic subduction zones: A direct comparison
600 between fossil petrological evidence (Rio San Juan Complex, Dominican Republic) and
601 numerical simulation: Lithos, v. 103, p. 106–137, doi: 10.1016/j.lithos.2007.09.003.
602 Krebs, M., Schertl, H.-P., Maresch, W.V., and Draper, G., 2011, Mass flow in serpentinite-
603 hosted subduction channels: P–T–t path patterns of metamorphic blocks in the Rio San Juan

mélange (Dominican Republic): Journal of Asian Earth Sciences, v. 42, p. 569–595, doi: 10.1016/j.jseaes.2011.01.011.

Lardeaux, J.-M., 1981, Evolution tectono-metamorphique de la zone nord du Massif de Sesia-Lanzo (Alpes occidentales): un exemple d'éclogitisation de croute continentale: Paris VI.

Lardeaux, J.-M., 2014, Deciphering orogeny: a metamorphic perspective. Examples from European Alpine and Variscan belts: Part I: Alpine metamorphism in the western Alps. A review: Bulletin de la Societe Geologique de France, v. 185, p. 93–114, doi: 10.2113/gssgfbull.185.2.93.

Lardeaux, J.-M., Gosso, G., Kienast, J.R., and Lombardo, B., 1982, Relations entre le métamorphisme et la déformation dans la zone Sesia-Lanzo (Alpes Occidentales) et le problème de l'é clogitisation de la croûte continentale: Bulletin de la Societé Géologique de France, v. 24, p. 793–800.

Lardeaux, J.-M., and Spalla, M.I., 1991, From granulites to eclogites in the Sesia zone (Italian Western Alps): a record of the opening and closure of the Piedmont ocean: Journal of Metamorphic Geology, v. 9, p. 35–59, doi: 10.1111/j.1525-1314.1991.tb00503.x.

Lemoine, M., and Trümpy, R., 1987, Pre-oceanic rifting in the alps: Tectonophysics, v. 133, p. 305–320, doi: 10.1016/0040-1951(87)90272-1.

Luoni, P., Rebay, G., Spalla, M.I., and Zanoni, D., 2018, UHP Ti-chondrodite in the Zermatt-Saas serpentinite : Constraints on a new tectonic scenario: American Mineralogist, v. 103, p. 1002–1005.

Malatesta, C., Crispini, L., Federico, L., Capponi, G., and Scambelluri, M., 2012, The exhumation of high pressure ophiolites (Voltri Massif, Western Alps): Insights from structural and petrologic data on metagabbro bodies: Tectonophysics, v. 568, p. 102–123,

doi: 10.1016/j.tecto.2011.08.024.

Malatesta, C., Gerya, T., Scambelluri, M., Federico, L., Crispini, L., and Capponi, G., 2012, Intraoceanic subduction of ``heterogeneous'' oceanic lithosphere in narrow basins: 2D numerical modeling: Lithos, v. 140--141, p. 234–251, doi: 10.1016/j.lithos.2012.01.003.

Manatschal, G., and Müntener, O., 2009, A type sequence across an ancient magma-poor ocean–continent transition: the example of the western Alpine Tethys ophiolites: Tectonophysics, v. 473, p. 4–19, doi: 10.1016/j.tecto.2008.07.021.

Manzotti, P., Ballèvre, M., Zucali, M., Robyr, M., and Engi, M., 2014, The tectonometamorphic evolution of the Sesia-Dent Blanche nappes (internal Western Alps): review and synthesis: Swiss Journal of Geosciences, v. 107, p. 309–336, doi: 10.1007/s00015-014-0172-x.

Marotta, A.M., Roda, M., Conte, K., and Spalla, M.I., 2018, Thermo-mechanical numerical model of the transition from continental rifting to oceanic spreading: the case study of the Alpine Tethys: Geological Magazine, v. 155, p. 250–279, doi: 10.1017/S0016756816000856.

Marotta, A.M., Spelta, E., and Rizzetto, C., 2006, Gravity signature of crustal subduction inferred from numerical modelling: Geophys. J. Int., v. 166, p. 923–938, doi: 10.1111/j.1365-246X.2006.03058.x.

Meda, M., Marotta, A.M., and Spalla, M.I., 2010, The role of mantle hydration into the continental crust recycling in the wedge region: Geological Society, London, Special Publications, v. 332, p. 149–172, doi: 10.1144/SP332.10.

Michard, A., Goffé, B., Chopin, C., and Henry, C., 1996, Did the Western Alps develop through an Oman-type stage? The geotectonic setting of high-pressure metamorphism in two contrasting Tethyan transects: Eclogae Geologicae Helvetiae, v. 89, p. 43–80.

650 Milano, P.F., Pennacchioni, G., and Spalla, M.I., 1988, Alpine and pre-Alpine tectonics in the
651 Central Orobic Alps (Southern Alps): Eclogae Geologicae Helvetiae, v. 81, p. 273–293.
652 Ogawa, Y., Mori, R., Tsunogae, T., Dilek, Y., and Harris, R., 2015, New interpretation of the
653 Franciscan mélange at San Simeon coast, California: tectonic intrusion into an accretionary
654 prism: International Geology Review, v. 57, p. 824–842, doi:
655 10.1080/00206814.2014.968813.
656 Penniston-Dorland, S.C., Kohn, M.J., and Piccoli, P.M., 2018, A mélange of subduction
657 temperatures: Evidence from Zr-in-rutile thermometry for strengthening of the subduction
658 interface: Earth and Planetary Science Letters, v. 482, p. 525–535, doi:
659 10.1016/j.epsl.2017.11.005.
660 Picazo, S., Müntener, O., Manatschal, G., Bauville, A., Karner, G., and Johnson, C., 2016,
661 Mapping the nature of mantle domains in Western and Central Europe based on
662 clinopyroxene and spinel chemistry: Evidence for mantle modification during an
663 extensional cycle: Lithos, v. 266, p. 233–263, doi: 10.1016/j.lithos.2016.08.029.
664 Piccardo, G.B., and Guarnieri, L., 2010, Alpine peridotites from the Ligurian Tethys: an updated
665 critical review: International Geology Review, v. 52, p. 1138–1159, doi:
666 10.1080/00206810903557829.
667 Pognante, U., 1989a, Lawsonite, blueschist and eclogite formation in the southern Sesia Zone
668 (Western Alps, Italy): European Journal of Mineralogy, v. 1, p. 89–104.
669 Pognante, U., 1989b, Tectonic implications of lawsonite formation in the Sesia zone (Western
670 Alps): Tectonophysics, v. 162, p. 219–227, doi: 10.1016/0040-1951(89)90245-X.
671 Pognante, U., Compagnoni, R., and Gosso, G., 1980, Micro-Mesostructural relatinships in the
672 continental eclogitic rocks of the Sesia-Lanzo Zone (Italian Western Alps): a record of

673 subduction cycle: Rendiconti della Società Italiana di Mineralogia e Petrologia, v. 36, p.
674 169–186.
675 Polino, R., Dal Piaz, G.V., and Gosso, G., 1990, Tectonic erosion at the Adria margin and
676 accretionary processes for the Cretaceous orogeny of the Alps: Mémoires de la Societé
677 Géologique de France, v. 156, p. 345–367.
678 Quinquis, M.E.T., and Buiter, S.J.H., 2014, Testing the effects of basic numerical
679 implementations of water migration on models of subduction dynamics: Solid Earth, v. 5, p.
680 537–555, doi: 10.5194/se-5-537-2014.
681 Rampone, E., Borghini, G., Romairone, A., Abouchami, W., Class, C., and Goldstein, S.L.,
682 2014, Sm-Nd geochronology of the Erro-Tobbio gabbros (Ligurian Alps, Italy): Insights
683 into the evolution of the Alpine Tethys: Lithos, v. 205, p. 236–246, doi:
684 10.1016/j.lithos.2014.07.012.
685 Ranalli, G., and Murphy, D.C., 1987, Rheological stratification of the lithosphere:
686 Tectonophysics, v. 132, p. 281–295, doi: 10.1016/0040-1951(87)90348-9.
687 von Raumer, J.F., Bussy, F., Schaltegger, U., Schulz, B., and Stampfli, G.M., 2013, Pre-
688 Mesozoic Alpine basements-Their place in the European Paleozoic framework: Geological
689 Society of America Bulletin, v. 125, p. 89–108, doi: 10.1130/B30654.1.
690 Raymond, L.A., 1984, Classification of mélanges, *in* Raymond, L.A. ed., Mélanges: Their
691 Nature, Origin, and Significance, Geological Society of America, doi: 10.1130/SPE198-p7.
692 Rebay, G., and Spalla, M.I., 2001, Emplacement at granulite facies conditions of the Sesia-Lanzo
693 metagabbros: an early record of Permian rifting? Lithos, v. 58, p. 85–104, doi:
694 10.1016/S0024-4937(01)00046-9.
695 Regis, D., Rubatto, D., Darling, J., Cenki-Tok, B., Zucali, M., and Engi, M., 2014, Multiple

696 Metamorphic Stages within an Eclogite-facies Terrane (Sesia Zone, Western Alps)
697 Revealed by Th-U-Pb Petrochronology: Journal of Petrology, v. 55, p. 1429–1456, doi:
698 10.1093/petrology/egu029.
699 Regorda, A., Roda, M., Marotta, A.M., and Spalla, M.I., 2017, 2-D numerical study of hydrated
700 wedge dynamics from subduction to post-collisional phases: Geophysical Journal
701 International, v. 211, p. 952–978, doi: 10.1093/gji/ggx336.
702 Roda, M., Marotta, A.M., and Spalla, M.I., 2010, Numerical simulations of an ocean-continent
703 convergent system: Influence of subduction geometry and mantle wedge hydration on
704 crustal recycling: Geochemistry, Geophysics, Geosystems, v. 11, p. n/a-n/a, doi:
705 10.1029/2009GC003015.
706 Roda, M., Marotta, A.M., and Spalla, M.I., 2011a, The effects of the overriding plate thermal
707 state on the slab dip in an ocean-continent subduction system: Compte Rendu Academie des
708 Sciences Paris, v. 343, p. 323–330, doi: 10.1016/j.crte.2011.01.005.
709 Roda, M., Marotta, A.M., and Spalla, M.I., 2011b, The effects of the overriding plate thermal
710 state on the slab dip in an ocean-continent subduction system: Comptes Rendus -
711 Geoscience, v. 343, p. 323–330, doi: 10.1016/j.crte.2011.01.005.
712 Roda, M., Regorda, A., Spalla, M.I., and Marotta, A.M., 2018, What drives Alpine Tethys
713 opening? Clues from the review of geological data and model predictions (C. Frassi, Ed.):
714 Geological Journal, p. 1–19, doi: 10.1002/gj.3316.
715 Roda, M., De Salvo, F., Zucali, M., and Spalla, M.I., 2018, Structural and metamorphic
716 evolution during tectonic mixing: is the Rocca Canavese Thrust Sheet (Italian Western
717 Alps) a subduction-related mélange? Italian Journal of Geosciences, v. 137, p. 311–329,
718 doi: 10.3301/IJG.2018.17.

719 Roda, M., Spalla, M.I., and Marotta, A.M., 2012, Integration of natural data within a numerical
720 model of ablative subduction: a possible interpretation for the Alpine dynamics of the
721 Austroalpine crust: Journal of Metamorphic Geology, v. 30, p. 973–996, doi:
722 10.1111/jmg.12000.
723 Rolland, Y., Lardeaux, J.-M., and Jolivet, L., 2012, Deciphering orogenic evolution: Journal of
724 Geodynamics, v. 56–57, p. 1–6, doi: 10.1016/j.jog.2011.09.004.
725 Rondenay, S., Abers, G.A., and Keken, P.E. Van, 2008, Seismic imaging of subduction zone
726 metamorphism: Geology, v. 36, p. 275–278, doi: 10.1130/G24112A.1.
727 Rosenbaum, G., Lister, G.S., and Duboz, C., 2002, Relative motions of Africa, Iberia and Europe
728 during Alpine orogeny: Tectonophysics, v. 359, p. 117–129.
729 Ruh, J.B., Le Pourhiet, L., Agard, P., Burov, E., and Gerya, T., 2015, Tectonic slicing of
730 subducting oceanic crust along plate interfaces: Numerical modeling: Geochemistry,
731 Geophysics, Geosystems, v. 16, p. 3505–3531, doi: 10.1002/2015GC005998.
732 Saccani, E., Dilek, Y., Marroni, M., and Pandolfi, L., 2015, Continental Margin Ophiolites of
733 Neotethys: Remnants of Ancient Ocean-Continent Transition Zone (OCTZ) Lithosphere
734 and Their Geochemistry, Mantle Sources and Melt Evolution Patterns: Episodes, v. 38, doi:
735 10.18814/epiiugs/2015/v38i4/82418.
736 Scarsi, M., Malatesta, C., and Fornasaro, S., 2018, Lawsonite-bearing eclogite from a tectonic
737 mélange in the Ligurian Alps: new constraints for the subduction plate-interface evolution:
738 Geological Magazine, v. 155, p. 280–297, doi: 10.1017/S0016756817000395.
739 Schmid, S.M., Fügenschuh, B., Kissling, E., and Schuster, R., 2004, Tectonic map and overall
740 architecture of the Alpine orogen: Eclogae Geologicae Helvetiae, v. 97, p. 93–117,
741 http://dx.doi.org/10.1007/s00015-004-1113-x.

742 Schmidt, M.W., and Poli, S., 1998, Experimentally based water budgets for dehydrating slabs
743 and consequences for arc magma generation: Earth and Planetary Science Letters, v. 163, p.
744 361–379, doi: 10.1016/S0012-821X(98)00142-3.
745 Schuster, R., and Stüwe, K., 2008, Permian metamorphic event in the Alps: Geology, v. 36, p.
746 603–606, doi: 10.1130/G24703A.1.
747 Spalla, M.I., Gosso, G., Marotta, A.M., Zucali, M., and Salvi, F., 2010, Analysis of natural
748 tectonic systems coupled with numerical modelling of the polycyclic continental lithosphere
749 of the Alps: International Geology Review, v. 52, p. 1268–1302, doi:
750 10.1080/00206814.2010.482737.
751 Spalla, M.I., Lardeaux, J.-M., Dal Piaz, G.V., Gosso, G., and Messiga, B., 1996, Tectonic
752 significance of Alpine eclogites: Journal of Geodynamics, v. 21, p. 257–285, doi:
753 10.1016/0264-3707(95)00033-X.
754 Spalla, M.I., De Maria, L., Gosso, G., Miletto, M., and Pognante, U., 1983, Deformazione e
755 metamorfismo della Zona Sesia – Lanzo meridionale al contatto con la falda piemontese e
756 con il massiccio di Lanzo, Alpi occidentali: Memorie della Società Geologica Italiana, v.
757 26, p. 499–514.
758 Spalla, M.I., Zanoni, D., Marotta, A.M., Rebay, G., Roda, M., Zucali, M., and Gosso, G., 2014,
759 The transition from Variscan collision to continental break-up in the Alps: insights from the
760 comparison between natural data and numerical model predictions: Geological Society,
761 London, Special Publications, v. 405, p. 363–400, doi: 10.1144/SP405.11.
762 Spalla, M.I., and Zulbati, F., 2003, Structural and petrographic map of the southern Sesia-Lanzo
763 Zone (Monte Soglio - Rocca Canavese, Western Alps, Italy): Memorie di Scienze
764 Geologiche, Padova, v. 55, p. 119–127.

765 Stampfli, and Hochard, 2009, Plate tectonics of the Alpine realm: Geol. Soc. London Spec.
766 Publ., v. 327, p. 89–111, doi: 10.1144/SP327.6.
767 Stöckhert, B., and Gerya, T.V., 2005, Pre-collisional high pressure metamorphism and nappe
768 tectonics at active continental margins: a numerical simulation: Terra Nova, v. 17, p. 102–
769 110, doi: 10.1111/j.1365-3121.2004.00589.x.
770 Stünitz, H., 1989, Partitioning of metamorphism and deformation in the boundary region of the
771 "Seconda Zona Diorito-Kinzigitica", Sesia Zone, Western Alps: Geologisches Institut der
772 Eidg. Technischen Hochschule und der Universität, Zürich, 244 p.
773 Turcotte, D.L., and Schubert, G., 2002, Geodynamics: Cambridge University Press, New York.
774 Le Voci, G., Davies, D.R., Goes, S., Kramer, S.C., and Wilson, C.R., 2014, A systematic 2-D
775 investigation into the mantle wedge's transient flow regime and thermal structure:
776 Complexities arising from a hydrated rheology and thermal buoyancy: Geochemistry,
777 Geophysics, Geosystems, v. 15, p. 28–51, doi: 10.1002/2013GC005022.
778 Vuichard, J.P., 1987, Conditions P–T du métamorphisme ante´alpin dans la seconde zone diorito-
779 kinzigitique (Zone Sesia-Lanzo, Alpes occidentales): Schweizerische Mineralogische Und
780 Petrographische Mitteilungen, v. 67, p. 257–271.
781 Wakabayashi, J., 2011a, Mélanges of the Franciscan Complex, California: Diverse structural
782 settings, evidence for sedimentary mixing, and their connection to subduction processes:
783 Geological Society of America Special Papers, v. 480, p. 117–141, doi:
784 10.1130/2011.2480(05).
785 Wakabayashi, J., 2011b, Subducted sedimentary serpentinite mélanges: Record of multiple
786 burial--exhumation cycles and subduction erosion: Tectonophysics, doi:
787 10.1016/j.tecto.2011.11.006.

Wakabayashi, J., 2015, Anatomy of a subduction complex: architecture of the Franciscan Complex, California, at multiple length and time scales: International Geology Review, v. 57, p. 669–746, doi: 10.1080/00206814.2014.998728.

Wheeler, J., and Butler, R.W.H., 1993, Evidence for extension in the western Alpine orogen: the contact between the oceanic Piemonte and overlying continental Sesia units: Earth and Planetary Science Letters, v. 117, p. 457–474, doi: 10.1016/0012-821X(93)90097-S.

Whitney, D.L., and Evans, B.W., 2010, Abbreviations for names of rock-forming minerals: American Mineralogist, v. 95, p. 185–187, doi: 10.2138/am.2010.3371.

Williams, P.F., and Compagnoni, R., 1983, Deformation and metamorphism in the Bard area of the Sesia Lanzo Zone, Western Alps, during subduction and uplift: Journal of Metamorphic Geology, v. 1, p. 117–140, doi: 10.1111/j.1525-1314.1983.tb00268.x.

Zanchetta, S., Malusà, M.G., and Zanchi, A.M., 2015, Precollisional development and Cenozoic evolution of the Southalpine retrobelt (European Alps): Lithosphere, v. 7, p. L466.1, doi: 10.1130/L466.1.

Zanoni, D., Bado, L., Spalla, M.I., Zucali, M., and Gosso, G., 2008, Structural analysis of the Northeastern margin of the tertiary intrusive stock of Biella (Western Alps, Italy): Boll. Soc. Geol. It. (Ital. J. Geosci.), v. 127, p. 125–140.

Zanoni, D., Rebay, G., and Spalla, M.I., 2016, Ocean floor and subduction record in the Zermatt-Saas rodingites, Valtournanche, Western Alps: Journal of Metamorphic Geology, v. 34, p. 941–961, doi: 10.1111/jmg.12215.

Zanoni, D., Spalla, M.I., and Gosso, G., 2010, Structure and PT estimates across late-collisional plutons: constraints on the exhumation of western Alpine continental HP units: International Geology Review, v. 52, p. 1244–1267, doi: 10.1080/00206814.2010.482357.

811 Zucali, M., 2011, Coronitic microstructures in patchy eclogitised continental crust: the Lago
812 della Vecchia Permian metagranite (Sesia-Lanzo Zone, Western Italian Alps): Journal of
813 The Virtual Explorer, v. 38.
814 Zucali, M., and Spalla, M.I., 2011, Prograde lawsonite during the flow of continental crust in the
815 Alpine subduction: Strain vs. metamorphism partitioning, a field-analysis approach to infer
816 5 tectonometamorphic evolutions (Sesia-Lanzo Zone, Western Italian Alps): Journal of
817 Structural Geology, v. 33, p. 381–398, doi: 10.1016/j.jsg.2010.12.006.
818 Zucali, M., Spalla, M.I., and Gosso, G., 2002, Strain partitioning and fabric evolution as a
819 correlation tool: the example of the Eclogitic Micaschists Complex in the Sesia-Lanzo Zone
820 (Monte Mucrone-Monte Mars, Western Alps, Italy): Schweiz. Mineral. Petrogr. Mitt., v. 82,
821 p. 429–454.
822 Zucali, M., Spalla, M.I., Gosso, G., Racchetti, S., and Zulbati, F., 2004, Prograde LWS-KY
823 Transition During Subduction Of The Alpine Continental Crust Of The Sesia- Lanzo Zone:
824 The Ivozio Complex: Journal of the Virtual Explorer, Electronic Edition, v. 16, p. 1–21.
825
826

827 Table 1 – Schematic overview of Alpine structural domains. Structural, metamorphic and
828 lithological characters synthetized in the table are widely discussed in Ernst, (1973); Brack,
829 (1981); Milano et al., (1988); Polino et al., (1990); Hunziker, (1992); Spalla et al., (1996);
830 Bousquet et al., (2004); Handy and Oberhänsli, (2004); Schmid et al., (2004); Berger and
831 Bousquet, (2008); Beltrando et al., (2010); Dal Piaz, (2010); Handy et al., (2010); Spalla et al.,
832 (2010); Roda et al., (2012); Rolland et al., (2012); von Raumer et al., (2013); Lardeaux, (2014);
833 Zanchetta et al., (2015); Roda et al., (2018); Filippi et al., (2018); Balestro et al., (2019).

834

	Helvetic Domain	Penninic Domain	Austroalpine Domain	Southalpine Domain
Tectonic Setting	External to the Penninic Front. This domain consists of Permian-Cenozoic cover sequences overlaying a Variscan basement, mainly characterized by pre-Alpine structural, metamorphic and stratigraphic signatures. Since the Palaeogene continental collision, Alpine tectonics reactivated the Mesozoic listric normal faults of the European passive margin into a thick-skin thrust system of basement and cover slices and decollement cover nappes.	The Penninic heterogeneous nappe system, occupying the axial part of the belt (comprised between the Penninic Front and the Periadriatic Lineament), is deformed and metamorphosed since Cretaceous, during Alpine oceanic subduction, exhumation and continental collision. It consists of a mélange of thin continental and oceanic basement and cover nappes. Continental slices mainly consist of Variscan metamorphic and igneous rocks overlaid by Permian-Mesozoic covers. Ophiolitic slices derive from the oceanic lithosphere of the sutured Tethys ocean.	The uppermost tectonic domain of the axial part of the Alpine belt consists of continental rocks overlying tectonically the Penninic stack of oceanic and continental rocks (ocean suture). It does not contain Mesozoic ophiolites but is infolded within them and the related Mesozoic sediments. Metamorphic conditions of Austroalpine do indicate in some places of the Western and Eastern Alps its implication in subduction processes since Upper Cretaceous to Paleocene. Subduction - collision structures are sealed by Oligocene-Miocene intrusive stocks.	Internal to the Periadriatic Lineament the Southalpine domain constitutes the hinterland of the Alpine belt. It is structured as a South-verging thrust system of continental basement and cover units since Cretaceous, locally displaying a weak Alpine metamorphic imprint.
Rocks	*Variscan basement* comprises well preserved to re-equilibrated eclogite-facies rocks, granulites, amphibolites, migmatitic metasediments and metagranitoids, marbles, peridotites and serpentinites. Eclogites and related HP-rocks generally occupy the core of amphibolite pods, embodied in migmatitic gneisses; HP-rocks predate Late Paleozoic intrusives and sediments. *Post Variscan cover rocks* comprise sandstones, conglomerate and volcanic rocks (Upper Carboniferous-Permian), Triassic carbonaceous sequences and Eocenic-Oligocenic volcano-sedimentary sequences.	Continental units comprise metaintrusives, paragneisses, micaschists, metabasics, marbles, migmatites, granulites, ultramafics that are Variscan protoliths widely reworked during Alpine subduction and collision. Oceanic units comprise metagabbros, metabasalts, widely serpentinized ultramafics, micaschists, quartzites, carbonaceous schists and marble+G1:G3s. The oldest intrusive photoliths have Middle Jurassic age.	Eclogites and ultramafics, metagranitoids and paragneisses, kyanite-schists and mylonites with minor metagabbros, marbles, manganiferous cherts, amphibolite, migmatites and Late Variscan granitoids are the protoliths of variably re-equilibrated Alpine metamorphic tectonites.	*Metamorphic basement* contains metapelites, amphibolites, meta-granitoids, quartzites, carbonaceous schists, marbles, migmatites, granulites, ultramafics and pegmatites. *Sedimentary covers* comprise Upper Carboniferous to Permian sandstones, conglomerates and volcanics, Triassic and Jurassic carbonaceous sediments, mainly terrigenous Cretaceous sediments and volcano-clastic Cenozoic sequences.
Variscan	Eclogites and spinel-bearing lherzolites developed during Variscan subduction, whereas during continental collision granulites and high-pressure migmatites originated. The late-orogenic collapse is testified by the occurrence of low-pressure migmatites and granulites and by late-Variscan granitoids.	Variscan subduction-related rocks, such as eclogites, are preserved as relict pods within mafic lenses of the Penninic polymetamorphic continental basement. Widespread occurrence of amphibolites and migmatites account for Variscan continental collision, whereas late Variscan granitoids are the markers of the late orogenic collapse.	Eclogites and garnet-bearing ultramafics in lenses, up to km-scale, within granulitic gneisses from Eastern Alps testify Variscan subduction. Eclogite-facies imprint predates the amphibolite imprint, well developed during continental collision. The eclogitized continental crust is evidence of the deep involvement of continent slices in the subduction zone, during a still active oceanic subduction or the early stages of the continental collision. Migmatites and Late Variscan granitoids are witnesses of continental collision and late orogenic collapse, respectively.	Intermediate pressure and intermediate temperature metamorphism (epidote amphibolite-facies imprint) of Devonian age is considered as the record of Variscan subduction. Carboniferous metamorphic ages (330-340 Ma) are interpreted as dating the amphibolite-facies T-peak, developed during Variscan collision. A late Variscan re-equilibration under greenschist-facies conditions is characterized by a high T/P ratio coherent with the thermal state of a late orogenic collapse.
Permian-Jurassic	Porphyritic dykes of andesitic composition intersect Variscan structures and rocks (Argentera Massif) as well as spilitic lava flows are associated with tuffs and mafic dykes of Triassic age (Pelvoux Massif): These magmatic products suggest the onset of Permian-Triassic lithospheric thinning.	During Jurassic oceanization follows continental rifting; gabbro emplacements, basaltic lava flows, deposit of siliceous and carbonaceous sediments occur. Mineral assemblages accounting for high temperature and low-pressure metamorphic conditions developed during oceanic metamorphism (e.g. Chennaillet).	Permian-Triassic amphibolites and granulites dominant in Western Alps, associated with spinel- and plagioclase-bearing ultramafics, Permian gabbros and Triassic pegmatites are the records of lithospheric thinning and continental rifting precuring the Tethys opening.	Permian-Triassic amphibolites, granulites, gabbros and ultramafics, together with basaltic lava flows, pegmatites and volcano-clastic Triassic sequences are the signatures of a lithospheric thinning precuring the Jurassic oceanization.
Alpine	Alpine structures consist of mylonitic belts, shear zones and open folds associated with foliations marked by greenschist- or epidote amphibolite-facies conditions. Metamorphic ages, ranging between 35 and 27 Ma, allow to interpret these structures as developed during the collisional stage.	*Continental units:* the subduction stage is testified by eclogites and garnet-bearing peridotites re-equilibrated under blueschist facies conditions. Widespread amphibolite facies imprint gives evidence of the collisional evolution, whereas low-pressure granulites and migmatites characterize mature collision and late-orogenic collapse. *Oceanic units*: eclogites and serpentinites, locally with ultra-high-pressure relics, are the marker of subduction. Re-equilibration under blueschist- or under amphibolite- facies conditions indicates that exhumation can occur during subduction or collision stages. During late Alpine times a greenschist re-equilibration occur. Some slices do not record the Alpine metamorphic imprint and show exclusively the metamorphic signatures of oceanic environment; therefore, they are interpreted as obducted (e.g. Chenaillet, Engadine Window).	Spinel- and garnet-bearing peridotites and eclogites develop in Western and Eastern Alps during subduction and are re-equilibrated under blueschist- (Western Alps, pre-collisional exhumation) or amphibolite- (Eastern Alps, sin-collisional exhumation) facies conditions. During late Alpine times a greenschist facies re-equilibration is heterogeneously recorded.	Alpine deformation and metamorphism are highly heterogeneous. Shear zones and open folds develop in the metamorphic basement and are associated with a basement-cover thrust system. Foliations are marked by greenschist- or prehnite pumpellyite-facies minerals. The northernmost thrust system is intersected by Cenozoic intrusives, therefore predating the collisional stage.

835

836

837 Table 2 - Material and rheological parameters used in the simulation. References: a) Ranalli and
838 Murphy, 1987; b) Afonso and Ranalli, 2004; c) Kirby, 1983; d) Haenel et al., 1988; e) Chopra
839 and Paterson, 1981; f) Dubois and Diament, 1997; Best and Christiansen, 2001; g) Roda et al.,
840 2011; h) Schmidt and Poli, 1998; i) Gerya and Stöckhert, 2005; j) Roda et al., 2012; k) Gerya
841 and Yuen, 2003; l) Meda et al., 2010.

	Continental crust	Upper oceanic crust	Lower oceanic crust	Dry mantle	Serpentinized mantle	Sediments	Sticky air
Rheology	Dry granite	Wet diabase	Diabase	Dry dunite	Serpentinite		
μ_0 (Pa s)	3.47e21	1.61e19	1.61e22	5.01e20	1.00e19	1.00e19	1.00e19
ρ_0 (kg m^{-3})	2640	2961	2961	3200	3000	2640	1000
K (W m^{-1} K^{-1})	3.03	2.1	2.1	4.15	4.15	3.03	0.026
H_r (μW m^{-3})	2.5	0.4	0.4	0.002	0.002	2.0	-
E (kJ mol^{-1})	38.43	103	103	130			
References	a,d,f,l	b,f,j,k,l	a,b,c,f,l	c,d,e,f,j,l	d,f,g,h,i	g,j	g,j

842

843

FIGURE CAPTIONS

Figure 1. (A) Tectonic sketch map of the Alpine chain. The gray ellipse indicates the location of the Sesia-Lanzo Zone shown in B. (B) Structural outline of the Sesia-Lanzo Zone in the Austroalpine domain of the Western Alps redrawn after Zucali et al. (2002). The gray ellipse locates the geological map of the Rocca Canavese Thrust Sheets (RCT) in panel C. (C) Interpretative geological map of the Rocca Canavese Thrust Sheets (RCT) redrawn after Roda et al. (2018). Coordinate system: Gauss-Boaga (Monte Mario 1).

Figure 2. P-T-d-t history of metabasics from the RCT redrawn after Roda et al. (2018). D1a represents the PT peak conditions inferred for the metagabbros and Jd-bearing glaucophanites, and D1b represents the PT peak conditions inferred for the Lws-bearing glaucophanites. D2 and D3 represent the PT conditions commonly recorded by the different types of metabasics during the development of the second and third groups of structures, respectively. The D2 and D3 structures are consistently recorded by the metapelites, metagranitoids, metabasics and serpentinites. (a) and (b) represent the two pre-D2 exhumation trajectories obtained for the metabasics of the RCT. The metamorphic facies are after Ernst and Liou (2008): GS=greenschist; Ep-A=epidote-bearing amphibolite; BS=blueschist; AM=amphibolite; EC=eclogite. Geotherms: Vi=stable geotherm (England and Thompson, 1984); 1="warm" subduction zones, 2="cold" subduction zones (Cloos, 1993).

Figure 3. Model setup after Regorda et al. (2017). The model domain is 1400 km wide and 710 km deep. The initial lithosphere thickness is 80 km and is defined by the 1227°C isotherm. The velocity boundary conditions correspond to a free slip condition along the bottom of the domain

867 and a fixed velocity along the top boundary. The vertical component of the velocity vector (U_y)
868 is fixed at 0 cm/yr on the right boundary along the entire lithospheric thickness (80 km depth)
869 and along the left side from 0 to 700 km depth. No slip conditions are imposed on the right and
870 left sides of the domain from the topographic surface to the upper boundary. Plate convergence is
871 simulated with a horizontal velocity of 3 cm/yr, and it is fixed along the bottom of the oceanic
872 crust and at the nodes of the numerical grid and distributed along a 45°-dipping plane from the
873 trench to a depth of 100 km. The thermal boundary conditions correspond to 0°C at the top of the
874 domain and 1227°C at the bottom. The initial thermal configuration corresponds to a uniform
875 purely conductive upper thermal boundary layer throughout the lithosphere (from 0 to 80 km
876 depth and from 0°C to 1227°C) and a uniform sublithospheric temperature of 1227°C (inset).
877 The temperatures are fixed along the left vertical sidewall, and a zero thermal flux is imposed on
878 the right side.
879
880 Figure 4. (A) D1a PT peak conditions extrapolated from markers of oceanic crust (dark gray
881 diamonds), continental crust (light gray diamonds) and trench sediments (white diamonds) from
882 20 to 45 Myr of oceanic subduction (from 80 to 55 Ma), and their evolution from 40 to 65 Myr
883 (50-35 Ma; dark gray, light gray and white circles, respectively). (B) D1b PT peak conditions
884 extrapolated from oceanic crust markers (dark gray squares), continental crust (light gray
885 squares) and trench sediments (white squares) from 20 to 45 Myr of oceanic subduction (from 80
886 to 55 Ma), and their evolution from 40 to 65 Myr (50-35 Ma; dark gray, light gray and white
887 circles, respectively).
888

889 Figure 5. P-T-t evolution of markers from peak conditions (D1a - light gray circles and D1b -
890 dark gray circles) to exhumation (white circles) in the subduction wedge (D3) during 65 Myr of
891 oceanic subduction compared to P-T-d-t paths obtained from the RCT metabasics (D1a, D1b, D2
892 and D3 areas and gray path). The entire metamorphic history of the RCT is fully reproduced by
893 the evolution of the numerical markers.
894
895 Figure 6. (A) Thermal states and depths of the markers with different lithological affinities
896 recording the P-T-t evolution shown in Figure 5 after 65 Myr of subduction (i.e., 35 Ma). The
897 tectonic mixture is composed of markers that belong to continental (green) and oceanic (black)
898 crust and trench sediments (yellow). (B) Locations of markers recording the P-T-t evolution
899 shown in Figure 5 after 65 Myr of subduction (red markers) with respect of all of the markers
900 involved in the model. The RCT tectonic mixture occurs as a narrow strip associated with
901 lithospheric mantle, serpentinized mantle and accreted sediments, and it marks the boundary
902 between the region that experienced subduction process (left) and the region that was not
903 involved in the subduction (right). White lines are the isotherms in degrees Celsius.
904
905 Figure 7: Conceptual representation of the evolution of RCT within the tectonic frame of
906 the Western Alps, compatible with the results of the numerical model of subduction (this work)
907 and collision (Regorda et al., 2017). (A) During subduction of the Ligurian-Piedmont ocean
908 below the Adria plate, the burial of oceanic, continental and sedimentary rocks occurred. (B)
909 While part of the subducted materials was recycled within the hydrated mantle wedge, the
910 metabasic blocks of RCT recorded different PT peak conditions (D1a and D1b metamorphic
911 conditions). (C) During exhumation, RCT blocks coupled together within a serpentinite-rich

matrix (D2 metamorphic conditions), that constituted the supporting material of the tectonic mélange of RTC. (D) The mélange exhumed as a single tectono-metamorphic unit until (E) the continental collision of the European plate. (F) The RCT marks the boundary between the orogenic wedge (Austroalpine and Penninic domains, in light blue) and the southern hinterland of the Alpine belt (Southalpine domain). The orogenic wedge is considered as a tectonic mixture of oceanic and continental rocks buried at different depths and exhumed to crustal levels, and part of the hydrated mantle wedge. In the inset, a conceptual cross section across the Western Alps (NW-SE) is shown (Polino et al., 1990; Spalla et al., 1996).

Figure 1

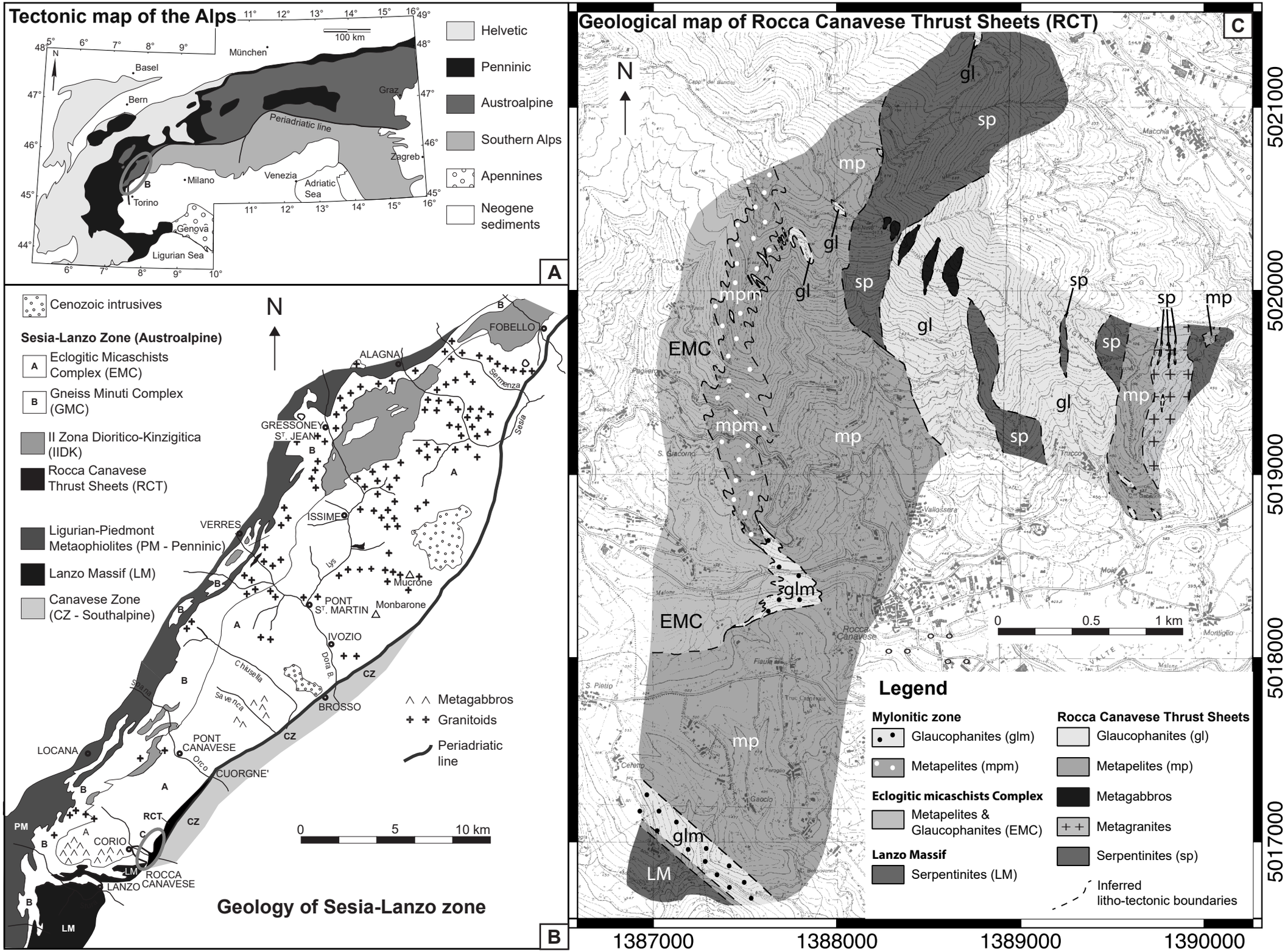
Tectonic map of the Alps
Helvetic
Penninic
Austroalpine
Southern Alps
Apennines
Neogene sediments
Periadriatic line
München
Basel
Bern
Graz
Zagreb
Milano
Venezia
Adriatic Sea
Torino
Genova
Ligurian Sea
100 km
A
Cenozoic intrusives
Sesia-Lanzo Zone (Austroalpine)
Eclogitic Micaschists Complex (EMC)
Gneiss Minuti Complex (GMC)
II Zona Dioritico-Kinzigitica (IIDK)
Rocca Canavese Thrust Sheets (RCT)
Ligurian-Piedmont Metaophiolites (PM - Penninic)
Lanzo Massif (LM)
Canavese Zone (CZ - Southalpine)
FOBELLO
ALAGNA
GRESSONEY ST. JEAN
ISSIME
VERRES
Mucrone
PONT ST. MARTIN
Monbarone
IVOZIO
BROSSO
PONT CANAVESE
LOCANA
CUORGNE'
CORIO
ROCCA CANAVESE
LANZO
Metagabbros
Granitoids
Periadriatic line
0 5 10 km
Geology of Sesia-Lanzo zone
B
Geological map of Rocca Canavese Thrust Sheets (RCT)
C
EMC
mp
mpm
sp
gl
glm
LM
0 0.5 1 km
Legend
Mylonitic zone
Glaucophanites (glm)
Metapelites (mpm)
Eclogitic micaschists Complex
Metapelites & Glaucophanites (EMC)
Lanzo Massif
Serpentinites (LM)
Rocca Canavese Thrust Sheets
Glaucophanites (gl)
Metapelites (mp)
Metagabbros
Metagranites
Serpentinites (sp)
Inferred litho-tectonic boundaries
1387000
1388000
1389000
1390000
5021000
5020000
5019000
5018000
5017000

Figure 2

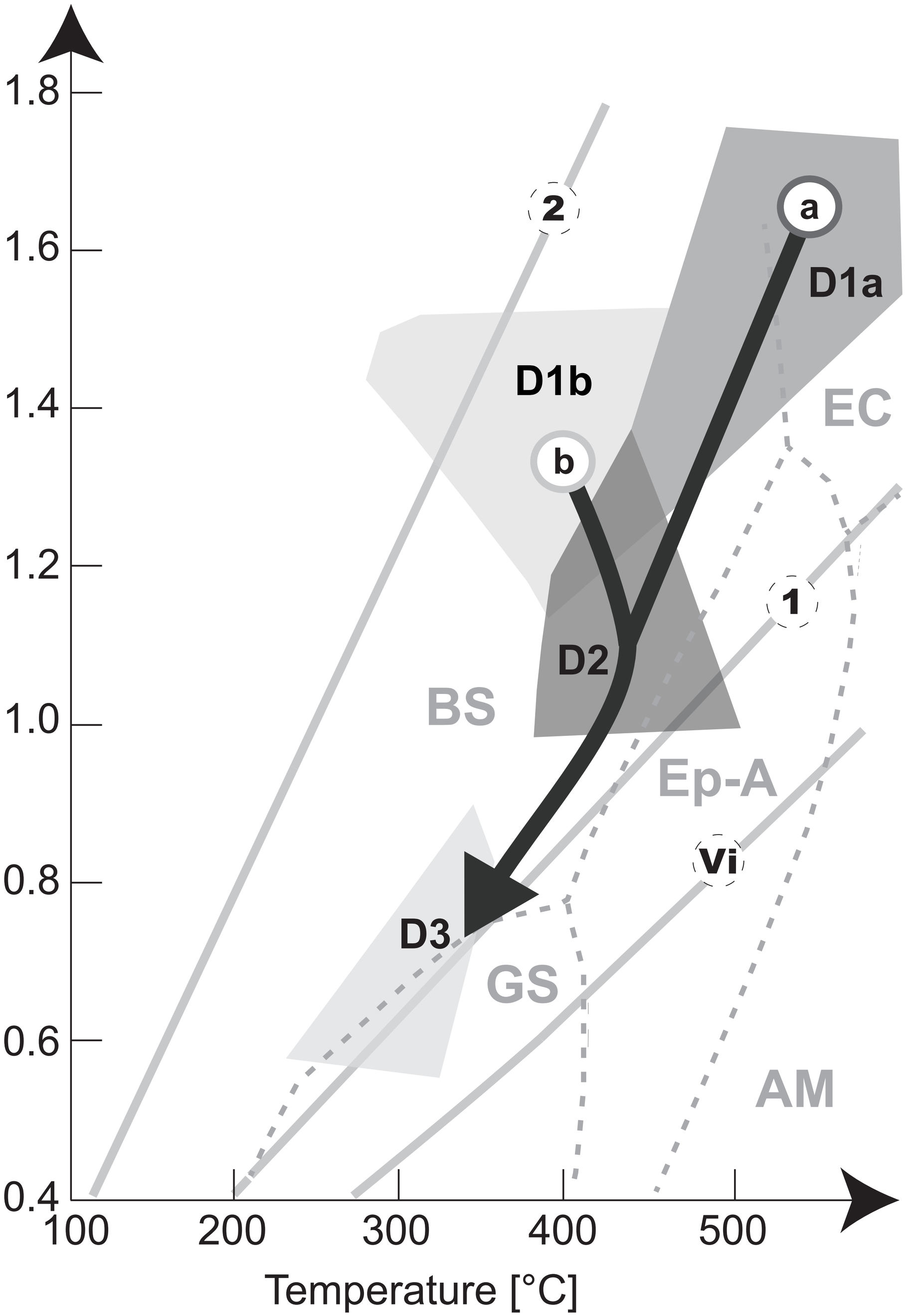
1.8
1.6
1.4
1.2
1.0
0.8
0.6
0.4
Pressure [GPa]
100
200
300
400
500
Temperature [°C]
2
a
D1a
D1b
b
EC
1
D2
BS
Ep-A
Vi
D3
GS
AM

Figure 3

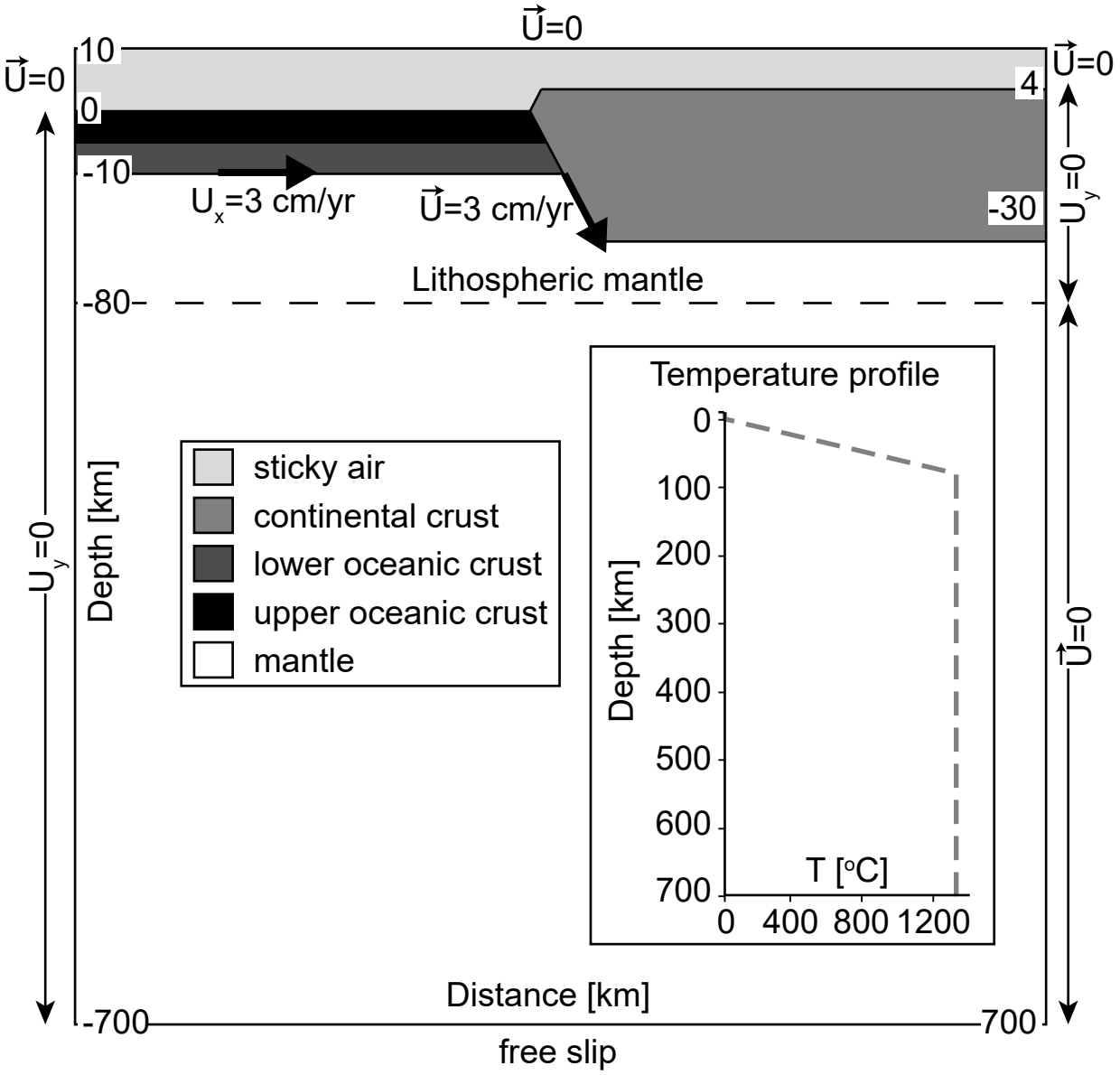
U=0
10
0
-10
4
-30
U=0
U=0
U=0
U=0
U_x=3 cm/yr
U=3 cm/yr
Lithospheric mantle
-80
sticky air
continental crust
lower oceanic crust
upper oceanic crust
mantle
Depth [km]
Temperature profile
0
100
200
300
400
500
600
700
Depth [km]
T [°C]
0 400 800 1200
Distance [km]
-700
700
free slip

Figure 4

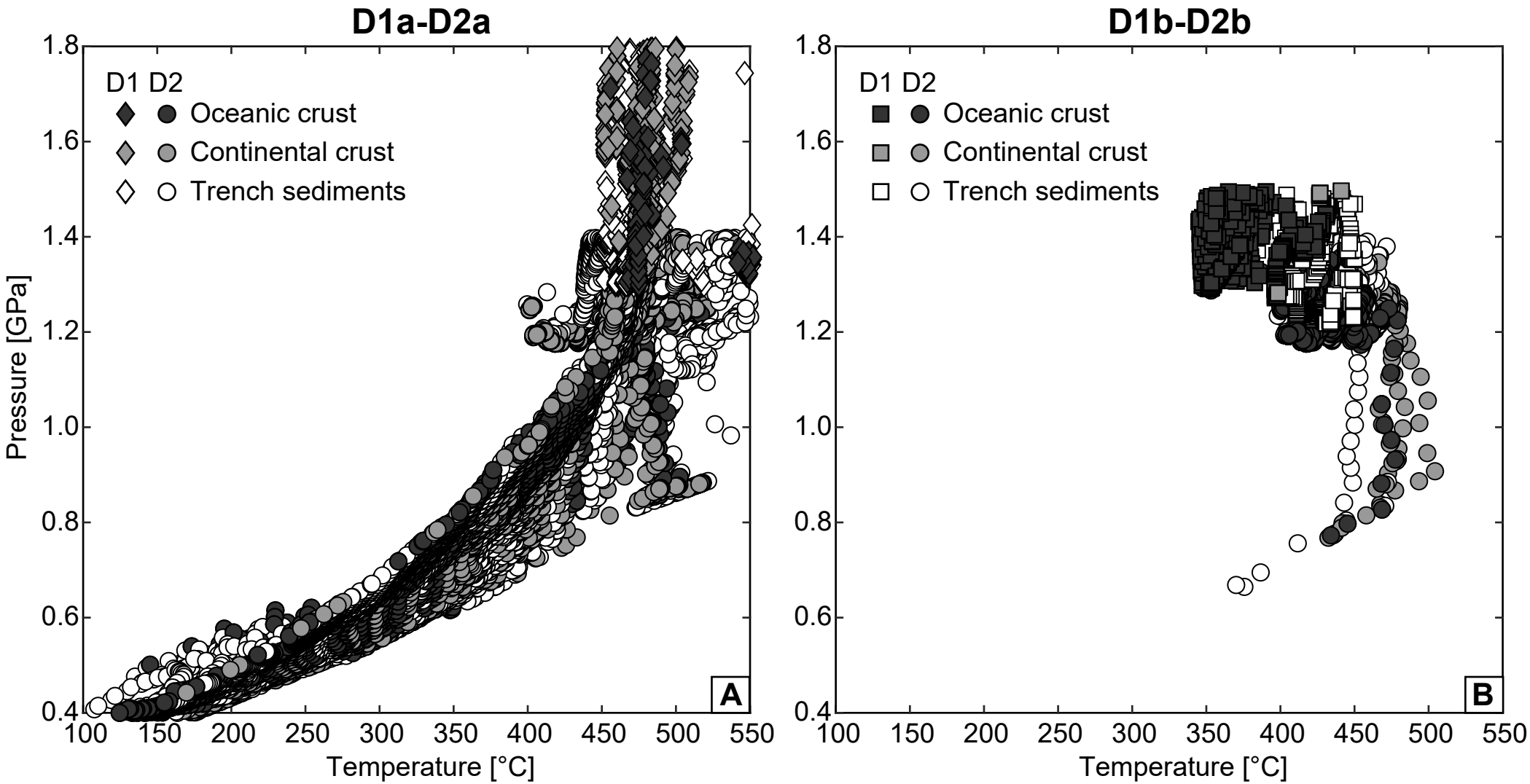
D1a-D2a
D1b-D2b
D1 D2
Oceanic crust
Continental crust
Trench sediments
Pressure [GPa]
Temperature [°C]
A
B
1.8
1.6
1.4
1.2
1.0
0.8
0.6
0.4
100
150
200
250
300
350
400
450
500
550

Figure 5

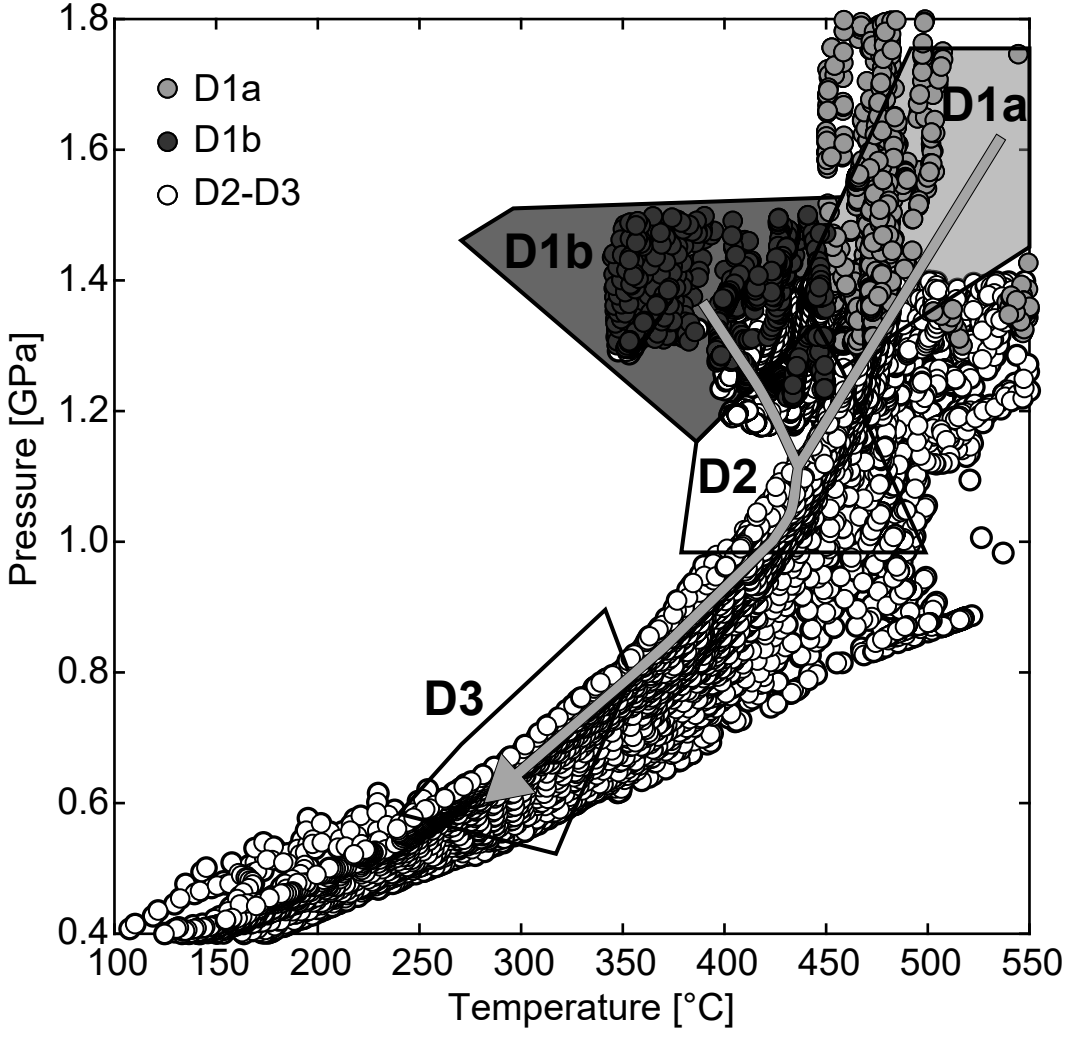
D1a
D1b
D2-D3
D1a
D1b
D2
D3
Pressure [GPa]
Temperature [°C]
1.8
1.6
1.4
1.2
1.0
0.8
0.6
0.4
100
150
200
250
300
350
400
450
500
550

Figure 6

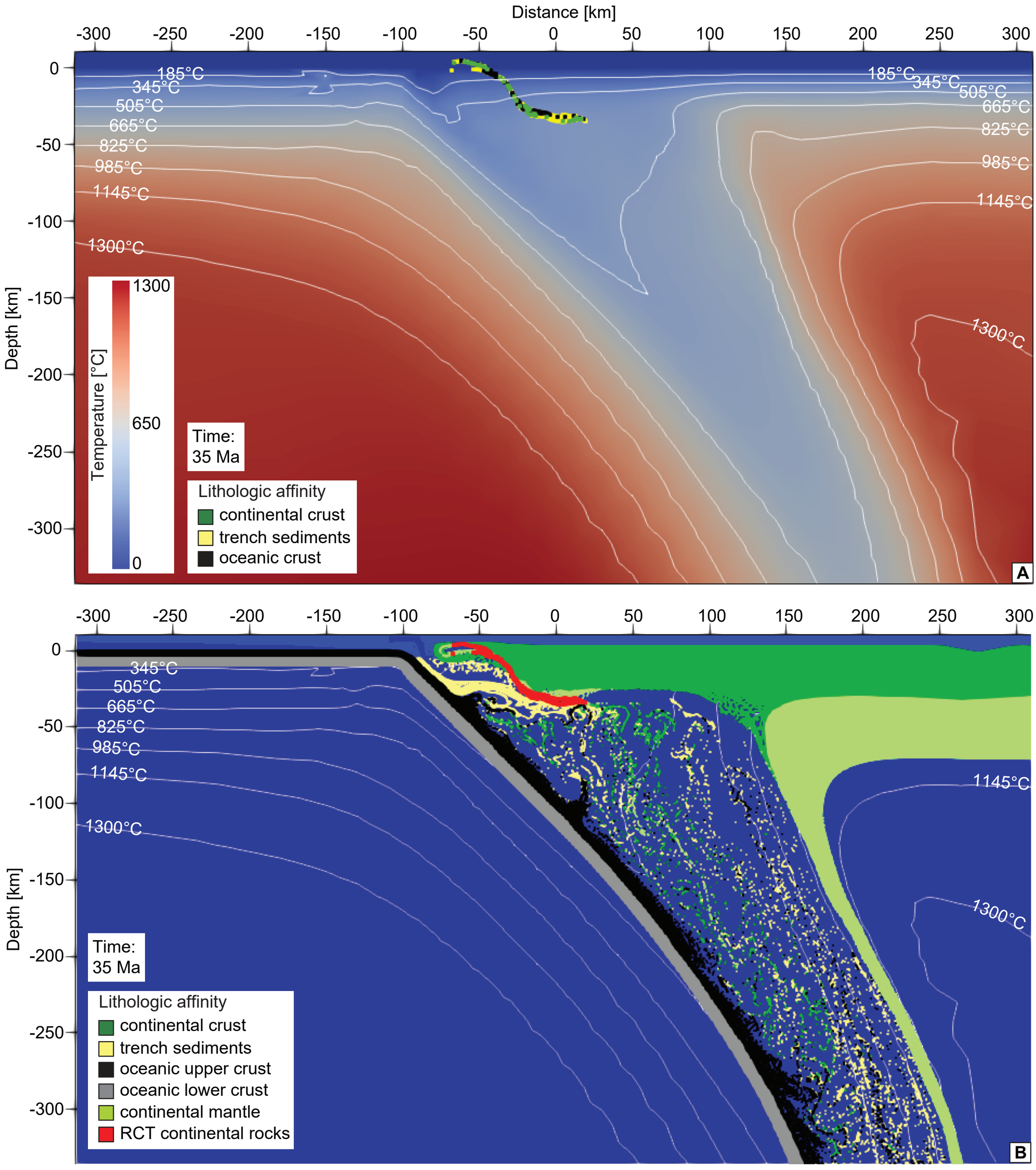
Distance [km]
-300
-250
-200
-150
-100
-50
0
50
100
150
200
250
300
Depth [km]
0
-50
-100
-150
-200
-250
-300
185°C
345°C
505°C
665°C
825°C
985°C
1145°C
1300°C
Temperature [°C]
1300
650
0
Time:
35 Ma
Lithologic affinity
continental crust
trench sediments
oceanic crust
A
Time:
35 Ma
Lithologic affinity
continental crust
trench sediments
oceanic upper crust
oceanic lower crust
continental mantle
RCT continental rocks
B

Figure 7

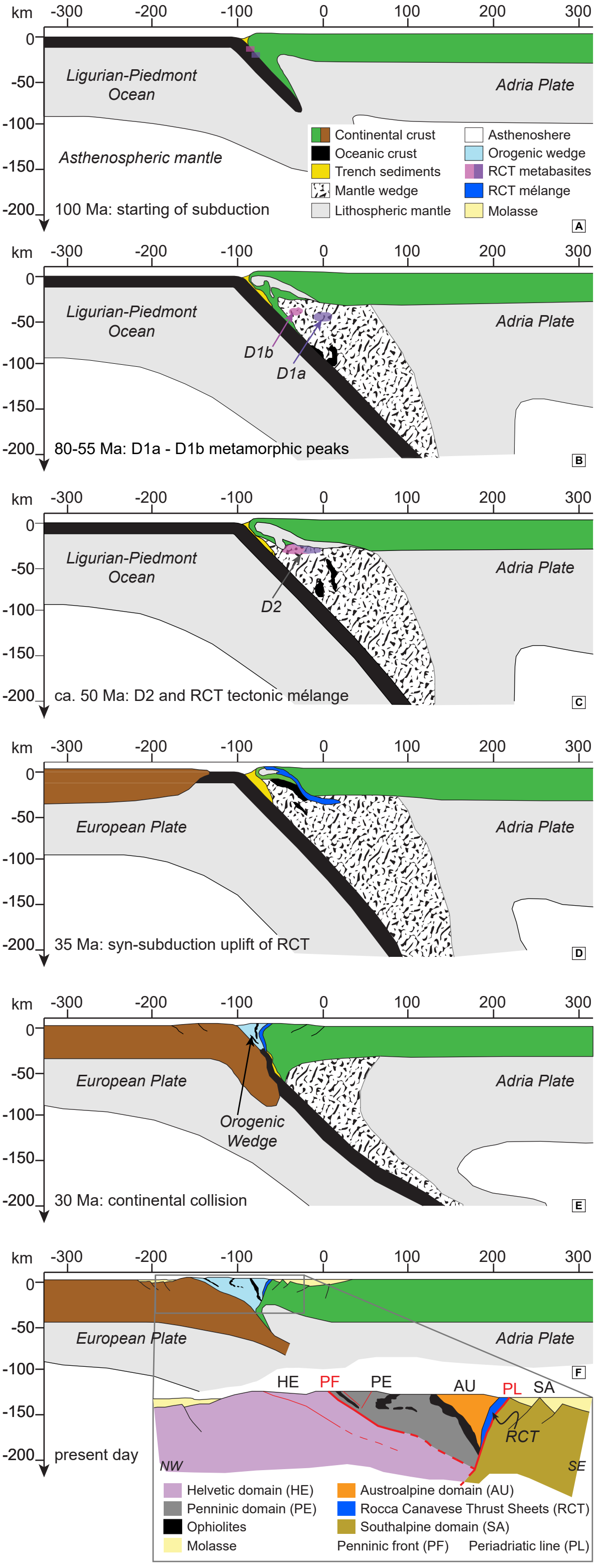
km
-300
-200
-100
0
100
200
300
0
-50
-100
-150
-200
Ligurian-Piedmont Ocean
Adria Plate
Asthenospheric mantle
100 Ma: starting of subduction
Continental crust
Oceanic crust
Trench sediments
Mantle wedge
Lithospheric mantle
Asthenoshere
Orogenic wedge
RCT metabasites
RCT mélange
Molasse
A
D1b
D1a
80-55 Ma: D1a - D1b metamorphic peaks
B
D2
ca. 50 Ma: D2 and RCT tectonic mélange
C
European Plate
35 Ma: syn-subduction uplift of RCT
D
Orogenic Wedge
30 Ma: continental collision
E
present day
F
HE
PF
PE
AU
PL
SA
RCT
NW
SE
Helvetic domain (HE)
Penninic domain (PE)
Ophiolites
Molasse
Austroalpine domain (AU)
Rocca Canavese Thrust Sheets (RCT)
Southalpine domain (SA)
Penninic front (PF)
Periadriatic line (PL)